https://doi.org/10.5194/tc-2020-243
Preprint. Discussion started: 22 October 2020

The Cryosphere Discussions
Open Access
EGU

Sudden large-volume detachments of low-angle mountain glaciers – more frequent than thought

Andreas Kääb[1], Mylène Jacquemart[2], Adrien Gilbert[3], Silvan Leinss[4], Luc Girod[1], Christian Huggel[5], Daniel Falaschi[6,7], Felipe Ugalde[8,9], Dmitry Petrakov[10], Sergey Chernomorets[10], Mikhail Dokukin[11], Frank Paul[5], Simon Gascoin[12], Etienne Berthier[13], Jeff Kargel[14,15]

[1] Department of Geosciences, University of Oslo, Norway
[2] Cooperative Institute for Research in Environmental Sciences, University of Colorado at Boulder, United States
[3] Université Grenoble Alpes, CNRS, IGE, Grenoble, France
[4] Institute of Environmental Engineering, ETH Zurich, Switzerland
[5] Department of Geography, University of Zurich, Switzerland
[6] Instituto Argentino de Nivología, Glaciología y Ciencias Ambientales, Mendoza, Argentina
[7] Departamento de Geografía, Facultad de Filosofía y Letras, Universidad Nacional de Cuyo, Mendoza, Argentina
[8] Geoestudios, San José de Maipo, Chile
[9] Departamento de Geología, Facultad de Ciencias Físicas y Matemáticas, Universidad de Chile, Santiago, Chile
[10] Faculty of Geography, M.V.Lomonosov Moscow State University, Moscow, Russia
[11] High-Mountain Geophysical Institute, Nalchik, Russia
[12] CESBIO, Université de Toulouse, CNES/CNRS/INRA/IRD/UPS, Toulouse, France
[13] LEGOS, CNES, CNRS, IRD, UPS, Université de Toulouse, Toulouse, France
[14] Department of Hydrology and Atmospheric Sciences, University of Arizona, Tucson, AZ, USA
[15] Planetary Science Institute, University of Arizona, Tucson, AZ, USA

Correspondence to: Andreas Kääb (kaeaeb@geo.uio.no)

Abstract.

The detachment of large parts of low-angle mountain glaciers, resulting in massive ice-rock avalanches, have so far been believed to be a unique type of event, made known to the global scientific community first for the 2002 Kolka Glacier detachment, Caucasus Mountains, and then for the 2016 collapses of two glaciers in the Aru range, Tibet. Since 2016, several so-far unknown glacier detachments have been discovered and described, and new ones have occurred. In the current contribution, we compile, compare and discuss 19 actual or possible large-volume detachments of low-angle mountain glaciers at nine different sites in the Caucasus, the Pamirs, Tibet, Alaska's St. Elias mountains, and the Southern Andes. Many of the detachments reached volumes in the order of 10–100 million m^3. Communalities and differences between the cases investigated suggest that a set of different conditions drives a transient combination of factors related to low basal friction, high driving

https://doi.org/10.5194/tc-2020-243
Preprint. Discussion started: 22 October 2020

The Cryosphere Discussions
Open Access
EGU

stress, concentration of shear stress, and low resistance to exceed stability thresholds. Particularly, soft bedrocks below the detached glaciers seem to be a common condition among the observed events, as they offer smooth contact areas between the glacier and its substratum while being prone to till-strength weakening and eventually basal failure under high pore-water pressure. Surface slopes of the detached glaciers range between around 10° and 20°, possibly on the one hand low enough to enable development of thick and thus large-volume glaciers, and on the other hand steep enough to allow critical basal stresses to build up. Most of the ice-rock avalanches resulting from the detachments in this study have a particularly low angle of reach, down to around 0.1 (apparent friction angle), likely due to their high ice content and connected liquefaction potential, the ready availability of soft basal slurries and large amounts of basal water, and the smooth topographic setting typical for glacial valleys. Low-angle glacier detachments combine elements, and likely also physical processes of glacier surges and ice break-offs from steep glaciers. The surge-like temporal evolution ahead of several detachments or their geographic proximity to other surge-type glaciers suggests the glacier detachments investigated can be interpreted as endmembers of the continuum of surge-like glacier instabilities. Though rare, glacier detachments appear more frequent than previously thought and disclose, despite local differences in conditions and precursory evolutions, the fundamental and critical potential of low-angle soft glacier beds to fail catastrophically.

1 Introduction

Eighteen years after the detachment of Kolka Glacier in the Russian Caucasus, the 17 July and 21 September 2016 detachments of two neighbouring glaciers in the Tibet's Aru range directed attention at a new type of glacier instability that had been rarely observed and little described before (Gilbert et al., 2018; Kääb et al., 2018; Tian et al. 2017). The detachment of Kolka Glacier on 20 September 2002 released a 130 10^6 m^3 of ice and rock that claimed ~120 lives. Situated on a dormant volcano, it was long assumed that the Kolka Glacier catastrophe was unique and specific to the glacier's location on Mt. Kazbek (Haeberli et al., 2004; Huggel et al., 2005; Drobyshev, 2006; Evans et al., 2009b). The Aru twin glacier detachments – which released 68 and 83 10^6 m^3 of glacier ice – have recently raised the questions of whether and where such events may have happened before or need to be expected in the future, which factors (including climate change) ultimately allow low-angle glaciers to detach from their bed in such a catastrophic manner, and what this means for mountain hazard management. Indeed, several detachments similar to the Aru events, though smaller in magnitude, have been detected since (Falaschi et. al., 2019; Paul 2019; Jacquemart et al., 2020).

In contrast to glacier detachments, an extensively studied, though still not fully understood type of glacier instability is represented by glacier surges. Characterized by unusually high ice-flow speeds of up to tens of metres per day over large parts of a glacier, glacier surges last weeks to several years (Harrison and Post, 2003; Jiskoot, 2011; Harrison et al., 2015). Clusters of surge-type glaciers are found in many mountain regions around the world (Sevestre and Benn, 2015). The lowering of basal

https://doi.org/10.5194/tc-2020-243
Preprint. Discussion started: 22 October 2020

66 glacier friction that is associated with surging involves abnormally high water pressure, change in the thermal regime, and/or responses of subglacial till to increasing shear stress and water input (Clarke et al., 1984; Kamb, 1987; Truffer et al., 2000;
68 Fowler et al., 2001; Murray et al., 2003; Frappe and Clarke, 2007; Sevestre et al., 2015; Benn et al., 2019).

A second, well-known type of glacier instability happens over a wide range of magnitudes, from icefalls at steep glacier fronts
70 to large ice avalanches, when partial or entire ice volumes suddenly break off from hanging glaciers that are typically steeper than around 30° (Alean, 1985; Huggel, 2009; Faillettaz et al., 2015). The latter empirical value from literature offers a slope
72 threshold to separate the definitions of ice avalanches from glacier detachments. Impacts associated with ice avalanches, which typically have volumes much smaller than 1 10^6 m^3, are usually limited to a few kilometres, unless the failed ice transforms
74 into a highly mobile mass flow through liquefaction and incorporation of wet sediments or liquid water in the path (Petrakov et al., 2008; Evans and Delaney, 2015). Failure conditions and triggering factors of such steep ice avalanches typically include
76 glacier geometry (steep ramp-type glaciers, bedrock edges), bedrock topography (e.g. convex bed), atmospheric events (e.g. temperature increase), strong accumulation rates, ice-thermal conditions (e.g. frozen base or changes therein), instabilities of
78 the underlying bedrock that take with them ice resting on it, or seismic events (Alean, 1985; van der Woerd et al., 2004; Huggel, 2009; Fischer et al., 2013; Faillettaz et al., 2015).

80 Our third type of glacier instability, a sudden large-scale detachment of a mountain glacier, is much less frequent than the two types above, but shows a mobility at least as high as ice avalanches combined with the large volumes typically involved in
82 glacier surges, and can thus constitute a severe threat to communities and settlements located in remote areas.

In general, mass movements that result from sudden slope failures in ice- or snow-rich mountain environments are often
84 particularly mobile, leading to strongly increased run-out distances compared to ice/snow-free conditions (Petrakov et al., 2008; Huggel, 2009; Schneider et al., 2011; Evans and Delaney, 2015). Frictional heating melts ice and snow components,
86 which are either part of the initial slope failure or incorporated along the avalanche path. Liquid water, embedded in the glacier and sediments before detachment, can amplify the avalanche mobility. Also ice and snow surfaces, in case the avalanche
88 travels over those, are able to reduce basal friction. Here, we define sudden large-volume glacier detachments through their actual initiation, while the eventually resulting ice-rock avalanches, or other types of mass flows, might be similar to those
90 resulting from other high-mountain slope instabilities. By terming these events *glacier detachments*, we follow the suggestion by Evans and Delaney (2015) who describe the Kolka case as large-scale detachment of a valley glacier. Other authors, for
92 instance, called these failure events glacier slides, in reference to landslides (Petrakov et al., 2008), or glacier collapses (Kääb et al., 2018).

94 Our following selection focusses on detachments (much) larger than 1 10^6 m^3 and from glaciers with surface slopes of lower than around 20°, i.e. focussing on glaciers from which large-volume detachments were so far typically not expected. In setting
96 these criteria, we are well aware that it can be reasonable to include other events beyond this coarse selection in other types of analyses, depending on the goal of the investigation. The main scientific purpose of this paper is to provide an overview of all

https://doi.org/10.5194/tc-2020-243
Preprint. Discussion started: 22 October 2020

known glacier detachment events, either by summarizing existing detailed studies, or by providing such details for the first time (see Suppl. Tab. S1 for existing studies and new contributions by the present work). We aim to show and discuss the relation of low-angle glacier detachments to glacier surges and the continuum of high-mountain ice and rock instabilities. The main applied purpose of our study is to make experts involved in high-mountain hazard management aware of the so far little recognized possibility for glacier detachments and to discuss related potential key indicators.

2 Ice-rock avalanches

Ice-rock avalanches can be the result of very different initial types of slope failures and event cascades. A wide range of magnitudes, avalanche compositions and impacts have been observed (Schneider et al., 2011). In this section, we exemplify the diverse characteristics of ice-rock avalanches and the resultant mass flows in order to contrast them to sudden large-volume detachments of mountain glaciers. Schneider et al. (2011) compiled a large inventory of ice-rock avalanches and analyzed the relation between avalanche mobility and volume, ice and water content, topography, as well as the presence of low-friction surfaces. We use their extensive data collection as background data set for our study, extended by events from Petrakov et al. (2008), who concentrated on an event type they term catastrophic glacier multi-phase mass movements. In Fig. 1, each event of this combined data set is plotted as a gray circle according to its horizontal reach (L), elevation difference (H) and detachment volume (V). The size of the circles in Fig. 1a indicates the event volumes. The ratio H/L is the apparent friction coefficient or the angle of reach, called also "Fahrböschung", calculated from the uppermost scarp of the slope failure to the lowermost part of the mass movement deposits.

The event collection of Fig.1 includes a wide range of ice-rock failure and mass movement types. Dark grey circles mark the following examples, standing out mainly by type, volume and angle of reach:

- In the 1970 Huascaran (Peru) event (a similar smaller event took place in 1962), a rock-wall failure triggered by a M7.9 earthquake, incorporated large amounts of ice from above and below it, leading to a highly mobile and far reaching rock-ice avalanche of 80 10^6 m^3 that claimed up to 20'000 lives (e.g., Evans et al., 2009a). In Fig. 1, we use the solid deposits of the avalanche to define its reach and elevation difference, neglecting that a subsequent water/mud flood travelled much further (indicated by * symbols in Fig. 1). The 1970 Huascaran avalanche is one of the largest, farthest reaching, and the by far deadliest known, stressing the full catastrophic potential of ice-rock avalanches.
- A rock failure in the Chilean Andes in 1987 incorporated ice, snow and water which transformed the avalanche into a debris flow of 15 10^6 m^3 that sped down the Estero Parraguirre valley and killed more than 37 people (Hauser, 2002). In our collection, this is the farthest-reaching event (lowest angle of reach; H/L ~0.12) that did not originate as a glacier detachment.
- The 1964/65 Allen Glacier event, Alaska, is an example for a very large rock avalanche, likely triggered by an earthquake, that was able to run out over an abnormally low angle because it landed on a glacier (Post, 1968). Neighbouring glaciers

https://doi.org/10.5194/tc-2020-243
Preprint. Discussion started: 22 October 2020

show similar rock deposits from the same time, and also later earthquakes caused comparable rock avalanches that travelled far over low-angle glaciers (e.g., Shugar et al., 2012).

- In 1895, 5 10^6 m^3 of at least partially cold-based ice sheared off 40°-steep bedrock of malm limestone underlying Altels Glacier in the Swiss Alps (glacier surface slopes indicated as numbers within the circles in Fig. 1a). The resulting ice avalanche rushed up the opposite side of the valley and thus did not reach its maximum runout distance (indicated by → symbols in Fig. 1; Faillettaz et al., 2011). The Altels event is an example of a very large, pure ice avalanche, stemming from the detachment of a very steep glacier. Until it sheared off, the glacier was probably held in place by transverse bedrock riegels and cold patches/zones where it was frozen to its bed (Wagner, 1996).
- A number of ice-rock avalanches have occurred from different locations on Iliamna volcano, Alaska, the last of which is documented for June 2019 (Toney et al., 2020). Failure surfaces were typically on the order of 40°, and volumes reached up to around 20 10^6 m^3 (Caplan-Auerbach and Huggel, 2007; Huggel et al., 2007). These events show that enhanced geothermal heat fluxes can be involved in causing ice-rock avalanches.

https://doi.org/10.5194/tc-2020-243
Preprint. Discussion started: 22 October 2020

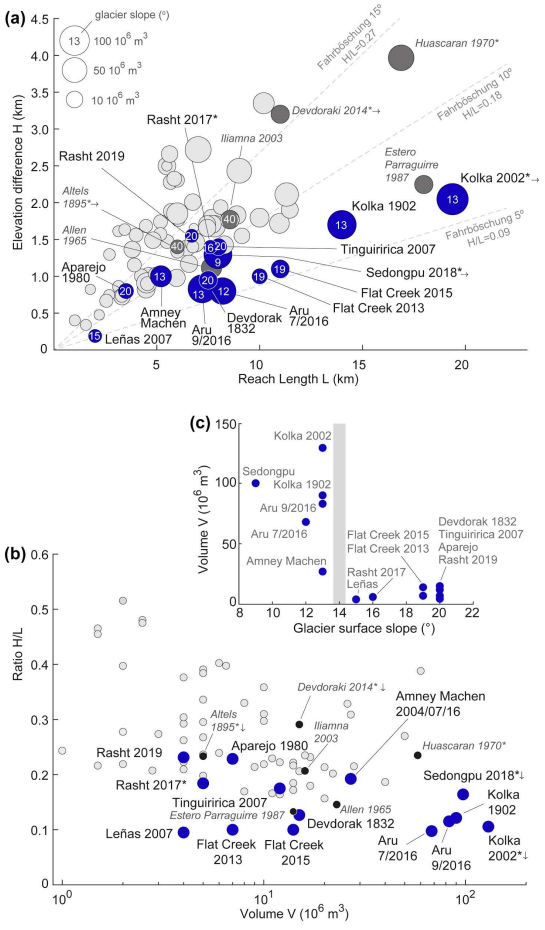

Figure 1: (a) Known avalanches of rock-ice mixtures plotted by elevation drop H versus Reach L. The event volumes are indicated by circle size (see legend). Blue circles are sudden large-volume detachments of low-angle mountain glaciers, with the surface slope of the detached glacier parts given in white numbers on the circles. The grey circles are other ice-rock avalanche events, with dark grey events mentioned specifically in the text to illustrate different event types collected in this figure. The diagonal dashed lines indicate the angle of reach, Fahrböschung, at 5°, 10° and 15°. (b) Events from (a) plotted by apparent friction coefficient (elevation drop H / Reach L) versus avalanche volume V. Note the logarithmic scale of the x-axes (volume). Most events stem from Schneider et al. (2011), extended by data from Petrakov et al. (2008) and the present study. * after the event name indicates that a mud or debris flow continued from the rock-ice avalanche deposits, which is not considered in the calculation of the reach. Arrows behind the event name indicate that the avalanche was stopped by some obstacle and would have ~~else~~ travelled further. The direction of the arrow indicates the direction in which the event symbol would have shifted in the plot without the obstacle. (c) Glacier detachment volume against glacier surface slope.

https://doi.org/10.5194/tc-2020-243
Preprint. Discussion started: 22 October 2020

3 Glacier detachment events

In the following, we summarize events that we categorize as glacier detachments, i.e. large-volume ice-rock avalanches from the sudden failure of low-angle parts of mountain glaciers (blue circles in Fig.1). Based on previously published findings from several of the events, we focus our descriptions specifically on disposition factors that could contribute to or hint at the presence of particularly low basal friction and high ~~shear~~ driving stresses. These factors include soft sediments, polythermal ice conditions, abnormal geothermal heat flux, high water input and basal water pressure, glacier surging, or significant steepening in surface slope. As it has been shown that ~~also~~ thermal conditions can also play a role in the detachments of glaciers (Gilbert et al., 2018; Jacquemart et al., 2020), we also try to evaluate permafrost conditions for each event.

We sort the following events by regions, and proceed within the regions from short summaries of well-documented events to more detailed descriptions of not or little studied cases. Discussions of individual events, e.g. regarding pre-satellite era events or a possible recurrence by glacier recovery, are included in the respective subsections, whereas the main discussion section 4 focuses on the overall comparison between events.

3.1 Mount Kazbek, Caucasus mountains

3.1.1 Devdorak, 18th century, 19th century, 2014

A number of glacier detachments and rock-ice avalanches happened around Mt. Kazbek at the border between Russia and Georgia. During the 18-19th centuries, surges of the Devdorak (Devdoraki in Georgian language) Glacier on the north-eastern flank of Mount Kazbek (Fig. 2; Tab.1) were moving along the Amilishka River (Kabakhi River in its lower part), which drains the glacier, in 1776, 1778, 1785, 1808, 1817, and 1832 (Zaporozhchenko and Chernomorets, 2004). On August 13, 1832, parts of the surging Devdorak glacier tongue detached and the subsequent ice-rock avalanche blocked the main Terek valley, an important transportation route between Russia and Georgia (Petrakov et al., 2008). Eyewitness of the 1832 event, engineer-captain Grauert estimated a volume of 15.5 10^6 $m^3$of ice and rock mass blocked the Dariali Gorge of the Terek valley (Zaporozhchenko and Chernomorets, 2004). The causes and mechanisms of this (and other) detachments are not well known, and vary throughout the literature. Ice-rock avalanching on the glacier, overloading and associated increase in subglacial water pressure could well have played a role.

Except for their source area, these at their time well known “Kazbek blockages” followed the same avalanche path as the 2014 Devdoraki event described below. Therefore, the 1832 event could instead have been similar to the 2014 event, starting as a rock failure rather than a surge (Chernomorets, 2014, Chernomorets et al., 2016).

In 2014, parts of a rock wall and overlying hanging glaciers failed from Mount Kazbek (Figs. 2-3). The resulting highly mobile rock-ice avalanche of 2-5 10^6 m^3 rushed down the Amilishka / Kabakhi Valley and blocked the main road between Russia and

https://doi.org/10.5194/tc-2020-243
Preprint. Discussion started: 22 October 2020

The Cryosphere Discussions
Open Access
EGU

Georgia, killing 9 people (Chernomorets et al., 2016; Tielidize et al., 2019). This event might also have had a longer runout (Fig. 1) but was stopped by a sharp 90°-turn at the confluence of the Devdoraki gorge and the Dariali (or Terek) gorge.

Currently, the entire narrow lower part of Devdorak Glacier has a surface slope of around 23°, its tongue closer to 17°. The volcanic nature of Mount Kazbek, the documentation of a number of violent mass flows from the mountain in the past (Chernomorets et al., 2007), field visits, and visual analysis of very high resolution satellite images and terrestrial photos all suggest highly erodible rock and an abundance of fine sediments at many places on Mount Kazbek. On all high-resolution satellite images available since around 2002 (GoogleEarth, Bing Maps, Maxar, Pleiades), Devdorak Glacier appears heavily crevassed, and is partly covered by fine sediments, likely deposited by mass movements from the surrounding mountain flanks. Since 2015, a glacier directly south of Devdorak Glacier has been overriding the main tongue of Devdorak glacier in a surge-like destabilisation, perhaps triggered by the 2014 Kazbek/Devdoraki rock-ice avalanche that overran it (Fig. 3). Possibly as a consequence of the tributary surge, Devdorak Glacier itself is currently also advancing (Dokukin et al., 2020). A 1-km global permafrost model (Obu et al., 2019), not particularly tuned for mountain permafrost, though, suggests the elevation of the Devdorak Glacier tongue is roughly at or below today's lower boundary of the discontinuous permafrost zone in the region.

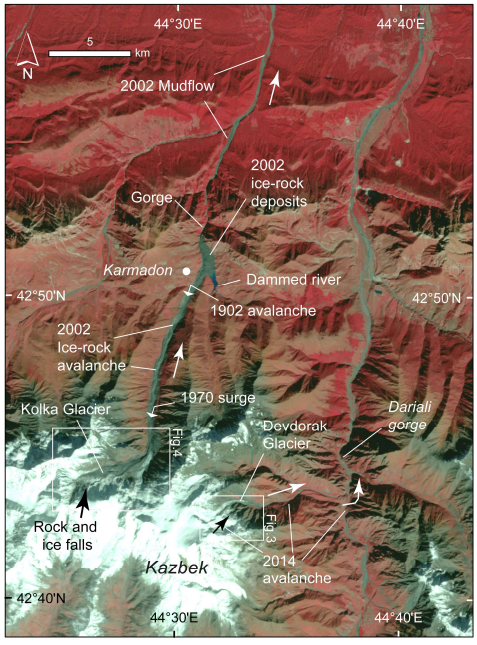

https://doi.org/10.5194/tc-2020-243
Preprint. Discussion started: 22 October 2020

The Cryosphere Discussions
Open Access
EGU

200 **Figure 2: Overview over Mount Kazbek, Russia/Georgia, Caucasus Mountains, with elements of the 2002 Kolka/Karmadon and 2014 Devdoraki rock-ice avalanches indicated. Satellite image: Landsat, 6 Oct 2002.**

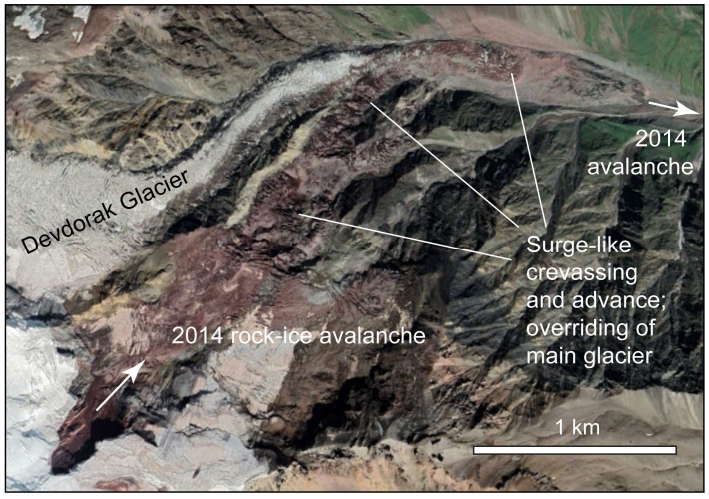

202 **Figure 3: Lower part of Devdorak Glacier and northeastern flank of Mount Kazbek. The position of the image section is indicated in Fig. 2. Satellite image: Pleiades, © Airbus, 19 Aug 2019.**

204

3.1.2 Kolka, 1902 and 2002

206 The 130 10^6 m^3 Kolka Glacier detachment (Figs. 2 and 4, Tab. 1) of 20 September 2002 has been described and discussed in a number of studies (Haeberli et al., 2004; Kotlyakov et al., 2004; Huggel et al., 2005; Drobyshev, 2006; Evans et al., 2009b).
208 During these investigations, it became clear that a similar event must have already happened at least once, at the beginning of July 1902 (and probably also around 1700), whereby the glacier tongue detached after a roughly two-week long surge-like
210 advance. Heavy rain and snow melt may have played a role in triggering the 1902 advance. Damming or erosion by water could then have caused the actual detachment and subsequent rock/mud/ice flow (Drobyshev, 2006; Petrakov et al., 2008;
212 Kotlyakov et al., 2010b). The glacier surged again in autumn/winter 1969/1970 and advanced by 4 km with speeds of up to 220 m/day (Fig. 4), but without catastrophic consequences (Hoinkes, 1972; Rototayev et al., 1983). It is not known to us,
214 which differences in conditions, compared to 1902 and 2002, caused the glacier to not detach in 1970. Several other glaciers in the Caucasus are known to have surged in the past (Kotlyakov et al., 2010b). We found that Kolka Glacier had a low surface
216 slope of around 13° prior to the 2002 detachment. Evans et al (2009b) estimated a bed slope of 9° after the detachment. Over the course of several weeks before the 2002 detachment, perhaps triggered by earthquakes (Kotlyakov et al., 2004), heavy rock
218 and ice falls from the northern flank of the Kazbek massif deposited several 10^6 m^3 of material on the glacier. During this

https://doi.org/10.5194/tc-2020-243
Preprint. Discussion started: 22 October 2020

period of mass-wasting activity, the glacier changed in unusual ways: it bulged and became heavily crevassed (Fig. 4), it developed a scarp at the location of the later detachment, and supraglacial ponds formed (Kotlyakov et al., 2004; Evans et al., 2009b; Kotlyakov et al., 2010b). Unusually high geothermal heat fluxes underneath the glacier (fumaroles and sulphur smell were reported ~~in~~ from the glacier bed shortly after detachment), the impact energy of a large rock/ice fall, and successive loss of shear stress due to excess water pressure have been proposed as possible factors and ultimate triggers of the 2002 detachment (Kotlyakov et al., 2004; Evans et al., 2009b; Kotlyakov et al., 2010b). Similarly, the additional loading of Kolka Glacier from the rock and ice falls has more recently been proposed to have increased the basal shear stress until it exceeded a frictional threshold given by the glacier bed material, topography, and hydraulic conditions (Kääb et al., 2018). After the detachment, lakes were visible on the Kolka Glacier bed, pointing to the involvement of large amounts of subglacial water in the detachment. The high mean avalanche velocities of 50-80 m/s (Huggel et al., 2005) suggest availability of large amounts of water and/or saturated fine-grained till.

The Kolka Glacier tongue is, like Devdorak Glacier, roughly at the lower elevation of the regional discontinuous permafrost zone, and the glacier must have been temperate throughout, except for the likely polythermal, or even cold steep hanging glaciers avalanching from the northern flank of the Kazbek massif onto its surface. The ice-rock avalanche resulting from the 2002 detachment is described in detail in the above literature about the event, but we want to draw attention to the streamlined debris stripes, in the following called striations, that were visible in the detachment zone after the event (Fig. 4d; Huggel et al., 2005), because similar patterns have also been found in several of the other cases of this study. Currently, the detached glacier depression is refilling and the glacier is gaining mass again. The fast recovery of the glacier volume between the 1970 surge and 2002, and again after the 2002 detachment, is associated with Kolka Glacier's positive mass balance, which stands in stark contrast to the predominant strong glacier shrinkage in the Caucasus Mountains (Kutuzov et al., 2019; Zemp et al., 2019). Kolka Glacier had already reached almost 50% of its pre-detachment volume by 2017 and is projected to accumulate 60–70% of its pre-detachment volume by 2025 (Petrakov et al., 2018; Aristov et al., 2019).

https://doi.org/10.5194/tc-2020-243
Preprint. Discussion started: 22 October 2020

The Cryosphere
Discussions
Open Access
EGU

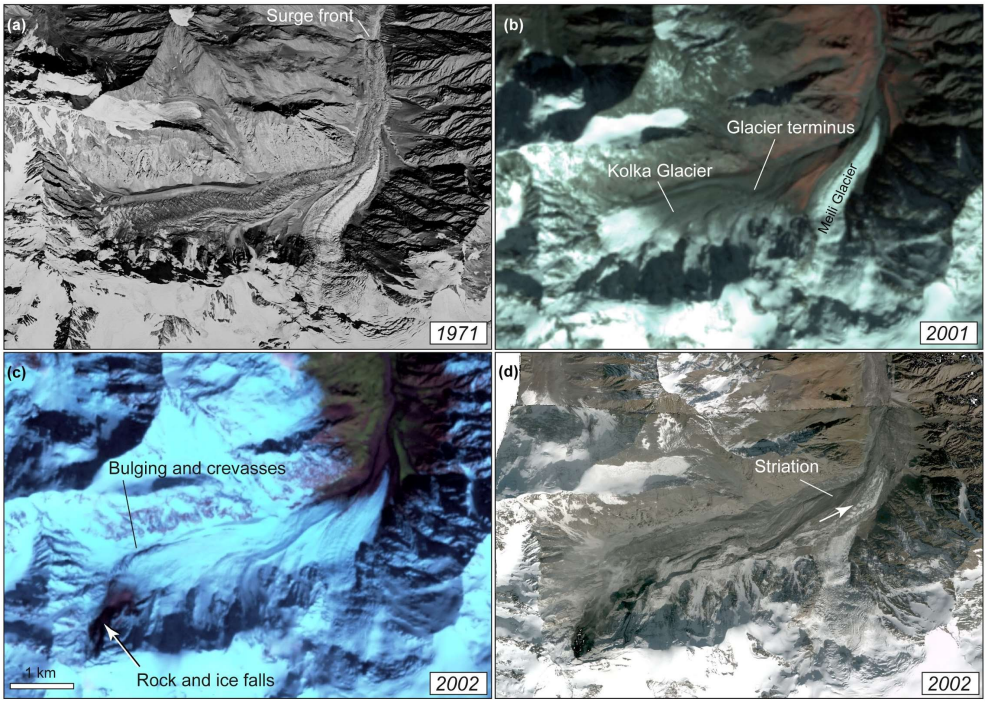

242 **Figure 4: Kolka Glacier, Mount Kazbek. (a) Kolka Glacier surged in 1969/70. Satellite image: Corona, 20 Sep 1971. (b)**
Landsat image, 3 Oct 2001. (c) Days and weeks before the 2002 detachment, rock and ice falls/avalanches were observed
244 **onto the glacier, and the left lateral margin of the glacier was bulged and heavily crevassed. Satellite image: Landsat,**
20 Sep 2002, a few hours before detachment. (d) Quickbird satellite image (© Maxar), 25 Sep 2002, 5 days after
246 **detachment. The position of the image sections is indicated in Fig. 2.**

248 ### 3.2 Rasht, Pamir/Tajikistan

In 2017 and 2019, two glacier detachment events happened on the north side of the Peter the First Range (or Petra Pervogo
250 Range, or Peter the Great Range), in the Pamir Mountains of Tajikistan. The resulting mass flows of both events flowed north into the Rasht Valley through which the Surkhob River flows that later forms the Vakhsh River (Fig. 5).

https://doi.org/10.5194/tc-2020-243
Preprint. Discussion started: 22 October 2020

252 **3.2.1 Event of 2017**

The 2017 event, first mentioned in Dokukin et al. (2019), happened between 10 and 11 July 2017 (Planet images). A glacier
254 of roughly 1000 m length and 240 m width detached (upper scarp ca. at 3600 m a.s.l) and the resulting ice-rock avalanche flowed down a narrow valley towards the village Tojikabod in the Rasht Valley (Figs. 5 and 6, Tab. 1). In satellite imagery
256 taken shortly after the event (Planet, Maxar), ice remains can be recognized over a horizontal distance of about 8 km, down to an elevation of about 2160 m a.s.l. Beyond this point, a considerable debris/mud flow must have continued for another 2 km
258 or so. The detached glacier had a surface slope of around 16° (High Mountain Asia DEM; Shean, 2017). We measured increased surface speeds of up to 5.8 m/day in early July 2017 (compared to a few dm/day in 2016; velocities from repeat
260 Planet data) and detected unusual lateral crevasses delineating the later detachment area in images from as early as May 2017 (Fig. 6). The glacier is likely not surrounded by permafrost (Obu et al., 2019).

262 To roughly estimate the event volume we derive the ice thickness along the center flow line of the glacier based on an estimated basal shear assuming a driving stress of 1.2 10^5 Pa as suggested for mountain glaciers, a slope of 16°, and a form factor of 0.8,
264 which then results in a thickness of around 60 m (Cuffey and Patterson, 2010). Multiplying half of this depth (i.e. assuming a triangular cross-section) with the detached area (ca. 200,000 m^2) gives a first volume estimate of roughly 6 10^6 m^3. Whereas
266 satellite images after detachment suggest that much of the glacier bed might actually have a triangular cross-section, it may have been more shallow in the lowermost and uppermost parts. As an order of magnitude, we suggest a detachment volume of
268 5 10^6 m^3 and assign a conservative error of ±1 10^6 m^3 to this estimate.

The cirque from which the 2017 event originated was also the source of other slope instabilities over recent years. Another
270 (much smaller) ice-rock avalanche from a neighbouring glacier occurred between 15 and 24 July 2016 (dates from Planet images), with a horizontal reach of roughly 5.5 km. A large debris flow descended the same valley in late August 2016, starting
272 from the same cirque, likely entraining deposits of the July 2016 avalanche, and reaching the Surkhob River 19.4 km downstream where it destroyed several buildings, bridges and agricultural fields.

274 **3.2.2 Event of 2019**

Between 2 and 3 August 2019 a second glacier, ca. 14 km to the west of the one that collapsed in 2017, detached (Figs. 5, 7).
276 This glacier was slightly smaller than the 2017 one, and had a surface slope of around 20°. The resulting ice-rock avalanche travelled north down a narrow valley towards the Rasht Valley, over a horizontal reach of 6.5 km and a vertical drop from
278 3350 (upper scarp) to 1850 m a.s.l. Superelevations of the ice-rock avalanche path of up to almost 200 m above valley bottom suggest high avalanche speeds (McClung, 2001). We estimated the detached volume in the same way as described for the 2017
280 event (section 3.2.1) and computed a volume of 4.5±1 10^6 m^3 (glacier area ca. 230,000 m^2; centreline depth 50 m). Based on pre- and post-event WorldView stereo DEMs Leinss et al. (2020) estimate a maximum erosion depth of 90 m and a detachment
282 volume of 8-9 10^6 m^3, i.e. significantly more than our rough general model.

https://doi.org/10.5194/tc-2020-243
Preprint. Discussion started: 22 October 2020

This glacier also showed increased sliding speeds and crevassing around the later detachment area for at least 2-3 weeks before the failure. For the end of July 2019 we found surface speeds of roughly 2.5 m/day, a marked increase compared to roughly < 0.1 m/day during 2017–2018 (repeat Planet data). The glacier did not show any visual signs of destabilisation between 2015 and 2018 (Planet images). In 2007 (Maxar; see Supplement) the glacier looked heavily crevassed, possibly an indication of a surge-like advance. This condition is still visible in Landsat data 5-6 years later, though less certain due to the lower resolution of Landsat data (no other data is available to us between 2007 and 2015). Landsat data also suggest that the glacier experienced a similar advance in the early 1990s. Under the limitation of the reduced spatial resolution of the Landsat data, however, we do not find signs of a large detachment event or large ice-rock avalanche. Nevertheless, we draw attention to a surprisingly vegetation-free landform visible downstream of the 2019 detachment in pre-event imagery (Fig. 8). The lack of vegetation, the streamlined microtopography, and zones of rough and chaotic microtopography that resemble avalanche or debris flow deposits (Fig. 8; Supplement), led us earlier to interpret this landform as a possible geomorphological imprint of an ice-rock avalanche (Kääb, 2019). Meanwhile, this landform has been overrun by the August 2019 ice-rock avalanche, leaving in parts similar new forms, and suggesting that the landform now buried could have stemmed from a similar detachment event, probably before 1961 (year of earliest Corona satellite image). Between the 1961 Corona images and very high-resolution images from just before the 2019 avalanche no significant changes are visible on the landform.

Very-high resolution satellite images over the Peter the First Range suggest abundance of weak bedrock and fine sediments. All over the range, signs after large debris flows, rock avalanches or ice-rock avalanches are visible in high resolution satellite images (Maxar, CNES/Airbus, Planet; Leinss et al, 2020). The Pamirs in general are known to be geomorphologically very active, with a number of associated hazards (Mergili et al., 2012; Gruber and Mergili, 2013; Strom and Abdrakhmatov, 2018) and a cluster of surge-type glaciers (Kotlyakov et al., 2008; Kotlyakov et al., 2010a; Gardelle et al., 2013; Sevestre and Benn, 2015; Lv et al., 2019). A number of glaciers in the Peter the Great Range are surging at the time of writing or have done so in the recent past (Fig. 5). Didal Glacier (ca. 12° steep) surged during the winter 2015/16 and advanced by 2.5 km over a few months. In the valley below Didal Glacier we note lack of vegetation in the valley and landforms that could well stem from a former ice-rock avalanche. Kotlyakov et al. (2010a) mention a 2.2 km long ice avalanche from Didal Glacier in 1974. In comparison, the bottom of the valley through which the 2017 ice-rock avalanche descended (section 3.2.1) was partly tree covered before, suggesting that no event like the 2017 one has happened there in the recent past.

Even if not documented in detail in an internationally accessible format so far, to our best knowledge, both the 2017 and 2019 detachments and their downstream effects were very likely noted by the local communities as the lowermost ice/rock deposits stopped not far from settlements, agricultural fields, and pastures, and very-high resolution images (Maxar) show that flooding happened close to houses and two irrigation channel bridges were partially destroyed.

https://doi.org/10.5194/tc-2020-243
Preprint. Discussion started: 22 October 2020

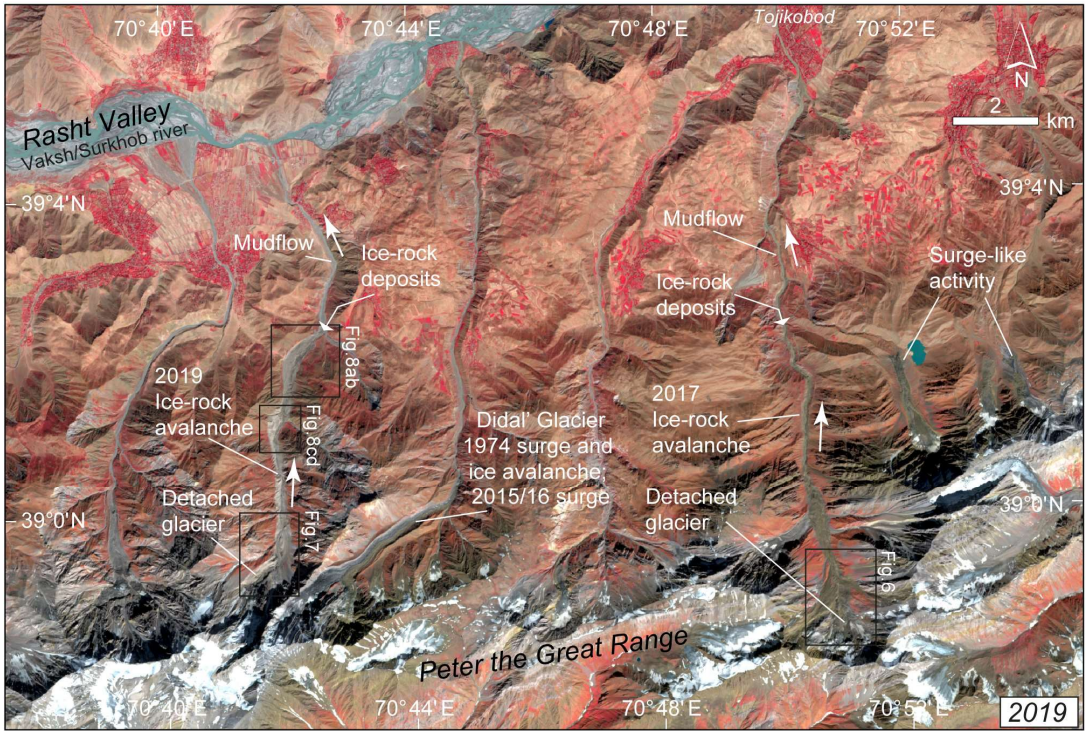

314

Figure 5: Rasht Valley and Peter the Great Range, Tajikistan. Locations of the 2017 and 2019 ice-rock avalanches are indicated. Satellite image: Sentinel-2 (EU Copernicus), 19 Sep 2019.

316

https://doi.org/10.5194/tc-2020-243
Preprint. Discussion started: 22 October 2020

The Cryosphere
Discussions
Open Access
EGU

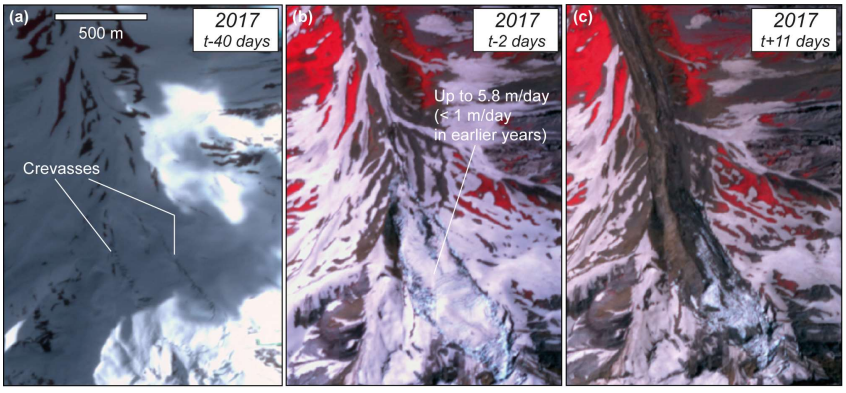

318

Figure 6: Planet images over the Rasht Valley glacier detachment of around 10 July 2017 (=t). (a) 31 May 2017, (b) 8 July 2017, (c) 21 July 2017. Abnormal marginal crevassing and enhanced speeds were visible several weeks before the detachment. See Fig. 5 for location. (Satellite images © Planet).

320

322

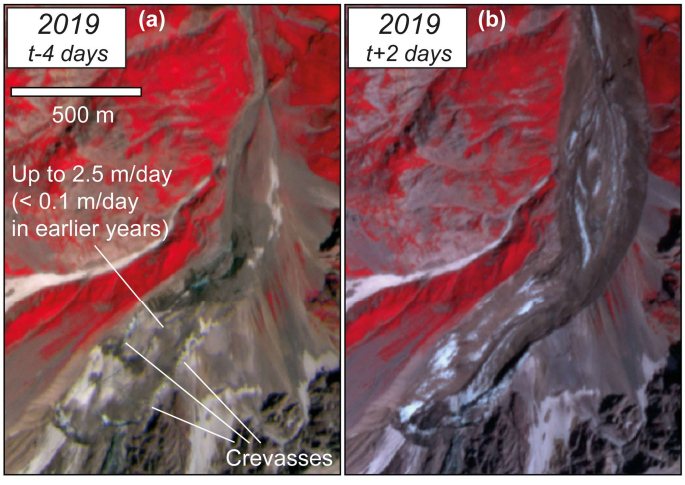

324 **Figure 7: Planet images over the Rasht Valley glacier detachment of around 2 Aug 2019 (=t). (a) 29 Jul 2019, (b) 4 Aug 2019. See Fig. 5 for location. (Satellite images © Planet).**

326

https://doi.org/10.5194/tc-2020-243
Preprint. Discussion started: 22 October 2020

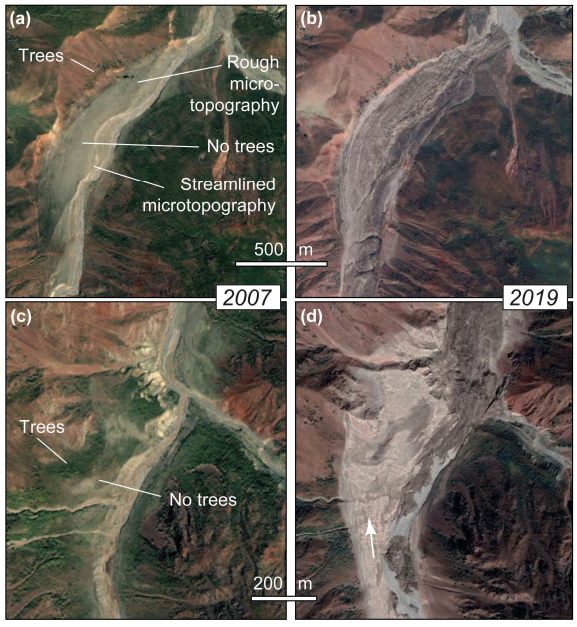

328

Figure 8: Location of the ~2 Aug 2019 Rasht Valley ice-rock avalanche. See Fig. 5 for image location. (a) and (c): 30 Jul 2007 (© Google Earth and Maxar). (b) and (d): 20 Aug 2019 (© Google Earth and CNES/Airbus). Before the 2019 event, traces of a potential former large mass flow were visible (lack of trees in the valley, sparse vegetation, striations).

332

3.3 Aru, 2016, western Tibet

334 On 17 July 2016, a massive volume of glacier ice detached from the lower part of an unnamed glacier in the Aru Range (Rutok County, China) in the western Tibetan Plateau (termed Aru-1). The fragmented ice mass ran out 6 km beyond the glacier 336 terminus, killing nine herders and hundreds of their animals, and reached the Aru Co lake (Tian et al., 2017; Kääb et al., 2018). The ice debris covered 8–9 km^2 and a volume of the detached glacier part of 68 10^6 m^3 was calculated. On 21 September 2016, 338 a second glacier (Aru-2) detached just a few km south of Aru-1 (Fig. 9). Similar to the July event, the glacier ice fragmented and transformed into a mass flow. The glacier debris in the second detachment covered 6–7 km^2 with a detached glacier volume 340 of 83 10^6 m^3. (Before-after elevation differences are available in Kääb et al. (2018)). The mean speeds of the Aru ice-rock avalanches were estimated to 30–50 m s^{-1}, with maximum speeds of 70–90 m s^{-1} (Kääb et al., 2018). (For a satellite image of 342 the current situation of the Aru glaciers and the deposits, see the Supplement).

https://doi.org/10.5194/tc-2020-243
Preprint. Discussion started: 22 October 2020


The Cryosphere Discussions
Open Access
EGU

Glaciers in the wider region around the Aru range are part of the Karakoram – West Kulun Shan – Eastern Pamir anomaly (Treichler et al., 2019) and experienced a slight increase in thickness of around 0.20– 0.30 m/a water equivalent since the early 2000s (Brun et al., 2017; Kääb et al., 2018). Positive mass-balances of the Aru glaciers (modeled based on ERA-interim reanalysis data; Kääb et al., 2018) and the widespread growth of endorheic lakes confirmed a precipitation increase in the region from the late 1990's on (Treichler et al., 2019). Driven by these positive mass balances, the two Aru glaciers underwent surge-like accelerations and mass transfers over years before the detachments (Gilbert et al., 2018; Kääb et al., 2018). In apparent contrast to the positive mass balances and the surge-like mass transfers, the Aru-1 and Aru-2 glaciers both retreated by around 500 m between 1970 and 2015.

Since at least 2011 and until 2014, the sections above the eventual detachment zones of both Aru glaciers subsided. Simultaneously, glacier sections below bulged upwards. The rates of elevation change derived for 2011–2014 indicate that a down-glacier mass transfer had already begun during the second half of the 2000s (Gilbert et al., 2018). A modelling study based on the observed elevation changes reconstructed changes in basal friction and horizontal velocity prior to the detachments (Gilbert et al., 2018). It showed that the two glaciers were close to their steady state geometry with no/little sliding until 2010. Thereafter, decreasing friction under the whole detachment area of Aru-1 and in more localized zones of Aru-2 started to trigger the surge-like mass transfer. Modelling the glaciers' thermal regimes revealed that the frictional changes likely occurred in temperate areas of the two glaciers and that stress concentration occurred at the cold-ice margins (Gilbert et al., 2018). The surge-like changes of basal friction under the Aru glaciers were thus likely not associated with a change of the glaciers' thermal regimes but rather with a change in friction due to increasing water pressure in the already temperate areas. During the instability development, basal shear stresses in the detachment area dropped by an order of magnitude, leading to significant stress concentrations at the detachment margins and in a few spots under the glaciers. These stress concentrations led to strongly enhanced crevassing at the glacier margins and the zone of the later ~~scrap~~ scarp head several months prior to the Aru-1 detachments. Fast-developing crevasses appeared only three weeks before the Aru-2 detachment and were discovered in satellite images in time to alert Chinese authorities.

The Aru glaciers are surrounded by continuous permafrost of -3 to -4 °C mean annual ground temperature (Obu et al., 2019). Field observations in the detachment and runout zones showed no presence of a hard-bed lithology beneath the glaciers, and no large boulders were observed anywhere in the runout paths. Rather, extensive deposits of soft, unconsolidated and fine-grained lithologies were identified. The Aru glaciers, situated in a region of positive or zero mass balances (Brun et al., 2017; Treichler et al., 2019) could well build up again to a size similar to the one before their 2016 collapses. Especially in the path of the Aru-1 avalanche, streamlined striations, not present before the event, are well visible at several locations in high-resolution satellite data (not shown).

↳ does this mean there is no evidence of a similar event in the more recent past?

https://doi.org/10.5194/tc-2020-243
Preprint. Discussion started: 22 October 2020

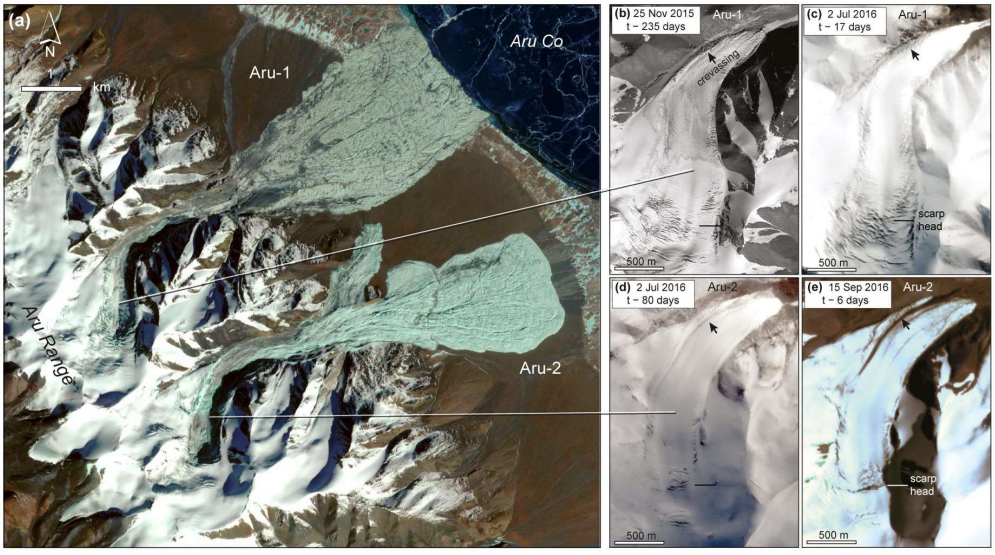

374 **Figure 9: Satellite images of the Aru glaciers, western Tibet, and their detachments. (a) Planet infra-red false-colour satellite image of 29 November 2016, after both glaciers collapsed (© Planet). (b) Enhanced crevassing on Aru-1 glacier**
376 **(SPOT7, © Airbus). Time *t* refers to detachment date (17 July 2016 for Aru-1, 21 September 2016 for Aru-2). Note the particular crevassing at the northern curve of the glacier. (c), Aru-1 (Planet). (d), Aru-2 (SPOT7, © Airbus). (e), Aru-**
378 **2 (© Planet), six days before collapse. The horizontal line in panels (b-e) indicates the scarp head positions of the later detachments.**

380

3.4 Amney Machen, 2004, 2007, 2016, and 2019, eastern Tibet

382 A sequence of surge-like advances, some of them ending in detachments of the glacier tongue, have been observed for a glacier in the Amney Machen mountain range, Eastern Tibet (Fig. 10, Tab. 1; Paul, 2019). The isolated mountain range is home to
384 several surging glaciers (Wenying, 1983). The first ice-rock avalanche happened between 26 January and 3 February 2004, and the involved volume was estimated to be 20-25 10^6 m^3, perhaps up to 36 10^6 m^3 according to a local information sign-
386 board (Paul, 2019). Three years later, between 23 September and 2 November 2007, a second detachment followed a surge-like advance, or surge-like recovery, of the glacier tongue that had detached in 2004. The 2007 detachment was considerably
388 smaller in volume than the one in 2004. A third detachment, also smaller than the 2004 one, occurred between 4 and 7 October 2016 (date from Planet images). Following this event, the glacier tongue started to recover again, and another small avalanche
390 occurred from it between 9 and 20 July 2019. Paul (2019) notes the weak rocks and fine sediments visible in the rock ribs in

which one, advance or recovery?

https://doi.org/10.5194/tc-2020-243
Preprint. Discussion started: 22 October 2020

the glacier's steep source area. The glacier recovered rapidly after each detachment, suggesting that it is largely nourished by ice and rock fall from the headwall, and that a rock/ice melange likely makes up the glacier tongue. The surface slope of the detaching lower part of the glacier is around 15°. The glacier lies in an area of continuous permafrost with ground temperatures in the order of -3 to -6°C (Obu et al., 2019). Streamlined striations in the avalanche path are visible in high-resolution satellite images (not shown).

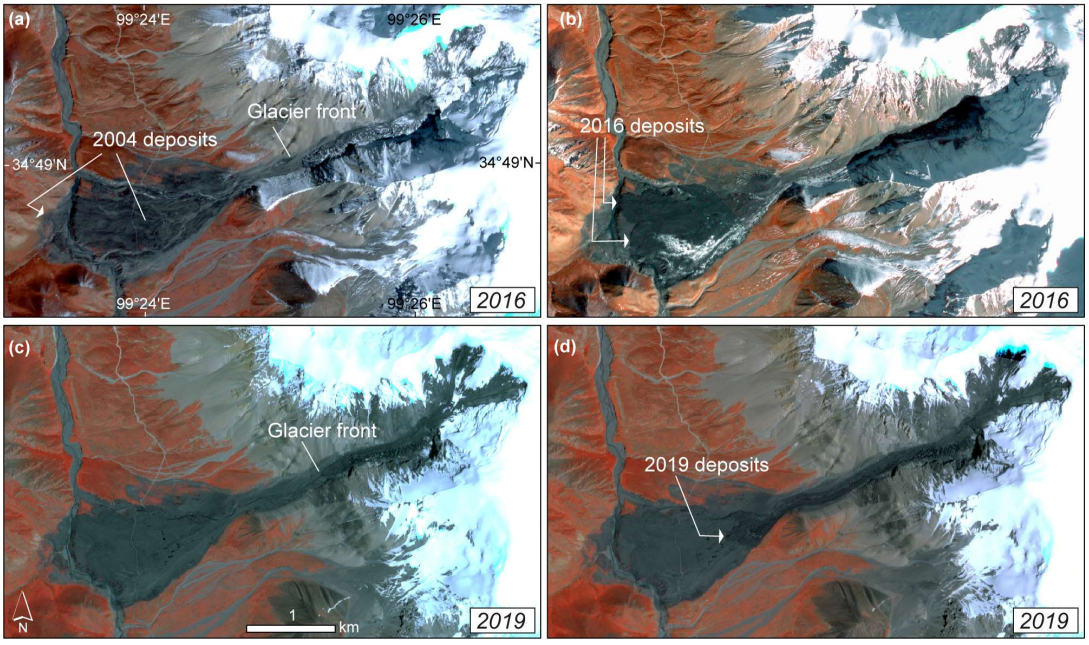

Figure 10: Unnamed glacier in the Amney Machen range, Tibet. Satellite images of (a) 2 Oct 2016, (b) 23 Oct 2016, (c) 9 Jul 2019, and (d) 25 Jul 2019. Detachments of the glacier tongue happened before (a), between (a) and (b), and between (c) and (d). (Satellite images © Planet).

3.5 Sedongpu/Gyala, 2018, south-eastern Tibet

During 2017 and 2018 the Sendongpu basin below the western flank of the Gyala Peri peak (7294 m.a.s.l.; Fig. 11) in south-eastern Tibet was the source of a series of large mass flows. Some of them dammed the Yarlung Tsangpo river, which posed a serious flood hazard to the upstream Gyalha village and large downstream areas, and triggered hazard management and

https://doi.org/10.5194/tc-2020-243
Preprint. Discussion started: 22 October 2020

investigations of the causes (Tong et al., 2018; Liu et al., 2019; Chen et al., 2020). The largest of the mass flows stemmed from the detachment of a large, low-angle glacier in 2018.

3.5.1 Events before 2018

In order to elucidate significant elements of the recent mass-flow history from the basin that might have conditioned the 2018 detachment and that are not documented in detail elsewhere, we start our description with the oldest satellite data available to us. In Corona satellite reconnaissance data of 8 Dec 1969, a narrowing in the Yarlung Tsangpo river where the Sendongpu valley joins the river, points to deposits from previous mass flows. However, trees on these deposits suggest no recent large mass flow activity. The main glacier in the basin, here called Sedongpu Glacier (Fig. 11), shows some signs of enhanced flow such as large crevasses. On Corona satellite data of 6 Nov 1974 the glacier has advanced some 800 m into steeper terrain. Fresh traces of a large mass flow are visible between the glacier front and the main Yarlung Tsangpo river, and fresh deposits seem to have covered or destroyed the forest on the older deposits in the river, but the main glacier is still in place. The glacier showed one single tongue in 1969, but had split into two tongues during its advance by 1974, a feature that it still exhibited in 2016. Chen et al. (2020) describe an ice avalanche from the Sedongpu basin that dammed the Yarlung Tsangpo river in 1968, but do not mention any other events before 2014. From our interpretation of the Corona satellite data there was either one more event(s) between 1969 and 1974, or the '1968' event actually happened a few years later. The next large mass flow (listed as ice avalanche in Chen et al. (2020) and debris flow in Tong et al. (2018); we interpret at least a large debris content) happened in 2014. The source of the mass flow must have been in the upper part of the main Sedongpu Glacier or its headwall, as both lateral moraines of the glacier were heavily eroded from the glacier side (RapidEye satellite data of 2013–2015). The glacier surface was not visibly changed along the glacier centre line, suggesting that the mass flow must have flowed along both glacier margins. Although difficult to determine in the satellite data available to us, the flow may have eroded the lowermost part of the glacier tongue.

Between 20 and 27 Oct 2017 (Planet and Sentinel-2 images) a huge rock avalanche started high up from the north ridge of Gyala Peri and ran over large parts of the Sedongpu basin and down to Yarlung Tsangpo, damming the river (Figs. 11 and 12). The event seems to have had a severe impact on Sedongpu Glacier. We generated two elevation models from 13 Nov 2015 Spot6 and 30 Dec 2018 Pleiades tri-stereo data that produced robust results despite the extreme topographic conditions. Differencing the two DEMs indicates that the October 2017 rock avalanche removed around 17 and 33 10^6 m^3 of material from two close-by but separated areas, respectively (Fig. 11c). If both failures happened as part of the same event, the total volume of 50 10^6 m^3 makes this one of the larger rock avalanches detected in recent decades. Based on visual inspection of satellite data, we consider it very likely that the avalanche also involved small glaciers from the west wall of Gyala Peri and incorporated ice from the surface of the glaciers lower down, as it ran over them. The Chinese seismic database registered two large 'landslide' events on 22 Oct 2017: A M3.2 event at 6:20 about 16 km west of Sedongpu and a M4.0 event at 6:22 directly at Sedongpu. Chen et al. (2020) and Tong et al. (2018) confirm that at least the latter signal stems from the Gyala Peri rock-

https://doi.org/10.5194/tc-2020-243
Preprint. Discussion started: 22 October 2020

ice avalanche. Subsequent satellite images suggest that the avalanche must have changed the surface of Sedongpu Glacier drastically. It covered the glacier and much of the basin with debris and dust. A small, surge-like lobe with ponds on it appeared at the transition between the headwall and the tongue of Sedongpu Glacier (Fig. 12, and GoogleEarth, BingMaps). The eastern tributary glacier to Sedongpu Glacier also showed a surge-like lobe (Sentinel-2, Planet, GoogleEarth). Driven by the geomorphological changes in the basin, a series of debris flows, some involving ice and likely nourished from the large amounts of unconsolidated debris left behind by the rock-ice avalanche, occurred after 22 Oct 2017 and into 2018 (Tong et al., 2018; Chen et al., 2020). The two 18 Nov 2017 M5.2 and M6.9 Linzhi/Milin/Nyingchi earthquakes, with epicentres only a few km from Sedongpu, may have contributed to triggering of the debris flows (Hu et al., 2019). Lastly, we report hundreds of small earthquakes recorded under the Gyala Peri massif in 2017 and 2018, most up to M2, some up to M3, which we have not analysed further in the present study (Chinese Earthquake Data Center, 2020).

3.5.2 Detachment in 2018

Following the 2017 rock-ice avalanche the main Sedongpu Glacier underwent drastic changes (Fig. 12). Ponds developed on its surface and along the margins. Surface velocities increased from a background velocity of ~0.3 m/d (ca. 100 m/a) in 2017 to 1–3 m/d end of January 2018, 10 m/d in mid-September 2018, and 25 m/d in mid-October 2018 (velocities derived from offset tracking in repeat Planet, Sentinel-1, and Sentinel-2 data). The glacier surface showed several crevassed bulges (Fig. 12b) in January 2018, and progressivley more crevasses appeared as the glacier tongue expanded (Fig. 12c). The lower, flat glacier part separated from the steep head wall. Between 19 Sep 2018 (last optical image due to later cloud cover) and 13 Oct 2018 (Sentinel-1) the glacier advanced by almost 1 km. On 17 or 18 October (Tong et al., 2018; Chen et al., 2020), the entire tongue of Sedongpu Glacier detached over a length of about 3.5 km (glacier width between 250 and 550 m) (Figs. 11 and 12). Planet images of 27 Oct 2018 and Chinese media images confirm that large amounts of ice blocked the Yarlung Tsangpo river (Fig. 11d). Parts of the emptied glacier bed filled up with enough ice debris that another mass flow originated from there on 29 Oct 2018. The dam in the Yarlung Tsangpo river was estimated to be roughly 40–60 10^6 m^3 in volume (Chen et al., 2020). Differencing our 2015 SPOT6 and 30 Dec 2018 Pleiades tri-stereo DEMs (Fig. 12d) shows two areas of distinct volume loss: around 80 10^6 m^3 are missing from the main branch of the glacier, and around 50 10^6 m^3 from its terminus and frontal moraine. An ASTER satellite stereo DEM of 11 Nov 2017 suggests that the volume loss over the glacier tongue and frontal moraine cannot have occurred before November 2017. From our data we cannot tell how much of the total 130 10^6 m^3 stems from the main first glacier detachment event of 17/18 Oct 2018, and how much from the 29 Oct 2018 event. However, satellite images indicate that the first event involved by far the largest volume. The detached glacier part had an overall slope of only 8–9°. According to Obu et al. (2019) it should have been several hundred meters below the regional permafrost limit, but cold or polythermal ice is certainly found in the west wall of Gyala Peri, and could theoretically be advected into the basal parts of the glacier near its tongue.

https://doi.org/10.5194/tc-2020-243
Preprint. Discussion started: 22 October 2020

Between 19 Sep and 26 Oct 2018 (Planet) a ~9 10^6 m^3 rock(-ice) avalanche (volume from 2015 SPOT6 and 2018 Pleiades tri-stereo DEM difference) originated from the south-western flank of Gyala Peri and likely reached Sedongpu Glacier (Fig. 11). The avalanche covered a small glacier below its starting zone which started a surge-like advance early 2018. Due to insufficient satellite data (cloud cover in optical data; low resolution and radar shadow in SAR data), though, we cannot tell if this avalanche happened before, during or after the 17/18 Oct 2018 glacier detachment, and could thus have triggered the glacier detachment. Seismic records are also inconclusive regarding the rock avalanche and the glacier detachment, with two dozens of M1–2 earthquakes recorded under the Gyala Peri massif between mid September and end of October 2018.

From all the evidence collected above, it seems very likely that the 22 Oct 2017 Gyala Peri rock avalanche, which travelled over the Sedongpu Glacier, primed the glacier for its detachment a year later, perhaps with additional influence of the18 Nov 2017 earthquakes, though the exact controlling mechanisms remain unclear. The effects that the ongoing mass-wasting activities from Gyala Peri had on Sedongpu Glacier can have been manyfold: additional loading on the glacier can have increased normal and shear stresses, and the 2017 rock avalanche and earthquakes could have mechanically weakened the glacier and its bed, potentially disrupting the subglacial drainage system. The large amounts of fine dust deposited on the glacier will likely have changed (enhanced?) its surface melt rates. Lastly, independent factors ~~like~~ high temperatures and precipitation amounts (Tong et al., 2018; Liu et al., 2019), associated with large water input into the glacier, could have complicated the changes caused by rock-avalanche impact. The supraglacial and glacier-marginal ponds, unusual on temperate glaciers (see Haeberli et al. 2002, Kääb et al. 2004), suggest that the glacier was under high internal water pressure. The bulging ice and the strong downstream gradient in surface velocities suggest that a surge-like instability first developed in the upper section of the low-angle part of the glacier. Just how this instability propagated down-glacier, whether by exerting pressure on the lower glacier from above, or by a propagation of exceptionally low basal friction values (Thogersen et al., 2019) remains unclear. High-resolution imagery and media photos of the glacier bed and detachment deposits, as well as the various debris flows that originated from the basin, suggest that the detached glacier rested on a soft bed with substantial amounts of fine material. The geology of the area is described as marble (Liu et al., 2019), which at least opens up the possibility of fine-grained sediments.

It remains to be seen to which extent the Sedongpu Glacier is able to rebuild, given the strongly negative mass balances in the region (Kääb et al., 2015; Brun et al., 2017; Treichler et al., 2019, Shean et al., 2020).

3.5.3 Zelunglung Glacier surge-like instabilities

The region around Sedongpu does not seem to host any obvious surge-type glaciers. However, the events at Zelunglung Glacier (29.62° N, 95.00° E; GLIMS G095018E29637N, RGI60-13.01428), 20 km south of Sedongpu, are worth mentioning. In 1950, 1968, and 1984 extraordinary instabilities propelled the glacier forward and blocked the Yarlung Tsangpo river (Zhang, 1992). The 1984 event seems to have involved only a smaller section of the glacier. Corona reconnaissance satellite images of 1969 show a massive advance (by about 4.5 km compared to 2018), but no detached glacier. However, the glacier had obviously

https://doi.org/10.5194/tc-2020-243
Preprint. Discussion started: 22 October 2020

overridden its frontal moraine, reaching almost down to Yarlung Tsangpo. Deposits, visually similar to those of ice-rock avalanches in general cover much of the main Yarlung Tsanpgo river bed on a length of about 2.5 km downstream measured from the confluence with the Zelunglung valley. Glacier advance rates of up to 1 km/h (!) are reported for the 1950 event (Zhang, 1992). Such rates are far above what is typical for surges and the glacier might have, at least in 1950, undergone an event close to a sudden detachment in the sense of the present contribution.

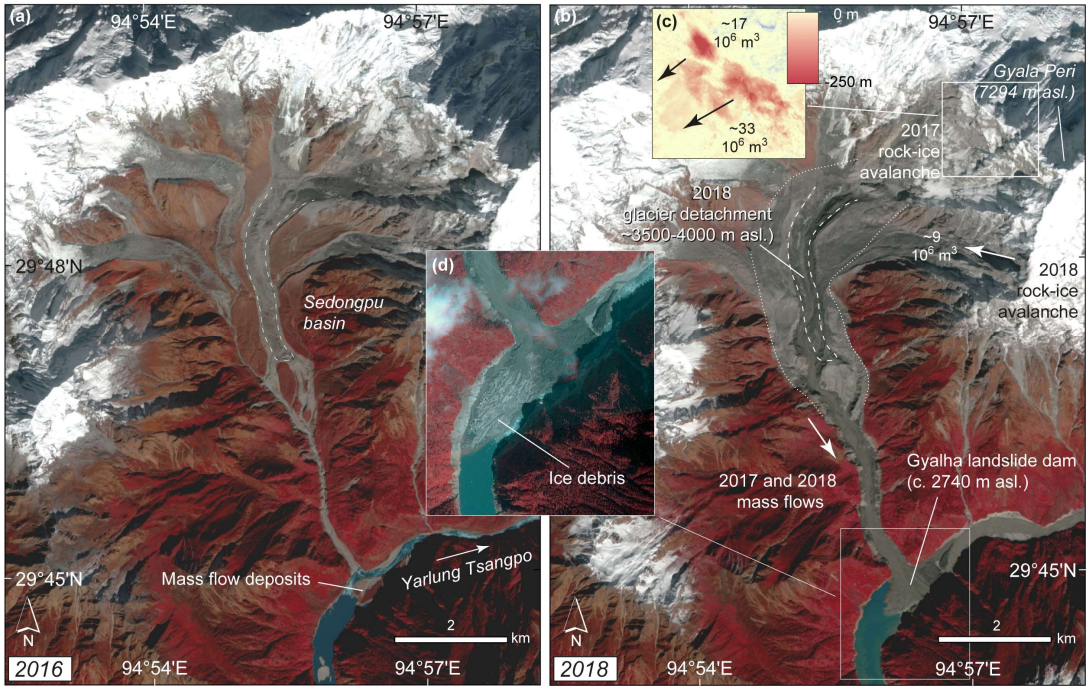

Figure 11: Location of the 17/18 Oct 2018 Sedongpu glacier detachment, south-eastern Tibet. (a) Sentinel-2 (EU Copernicus) image of 20 Nov 2016, before a series of mass flows happened that culminated in glacier detachment. Already earlier, mass flows from the basin have blocked the Yarlung Tsangpo river. (b) Sentinel-2 image of 31 Oct 2018 showing the area impacted by the 22 Oct 2017 rock avalanche from the Gyala Peri peak, and the 17/18 Oct 2018 glacier detachment. (c) Detail of elevation model differences between SPOT6 13 Nov 2015 and Pleiades 30 Dec 2018 tri-stereo data. Elevation losses amount up to 330 m, but the colour scale is saturated at -250 m. (d) Detail of the glacier detachment deposits in the main river (© Planet; image of 27 Oct 2018, 10 days after detachment).

https://doi.org/10.5194/tc-2020-243
Preprint. Discussion started: 22 October 2020

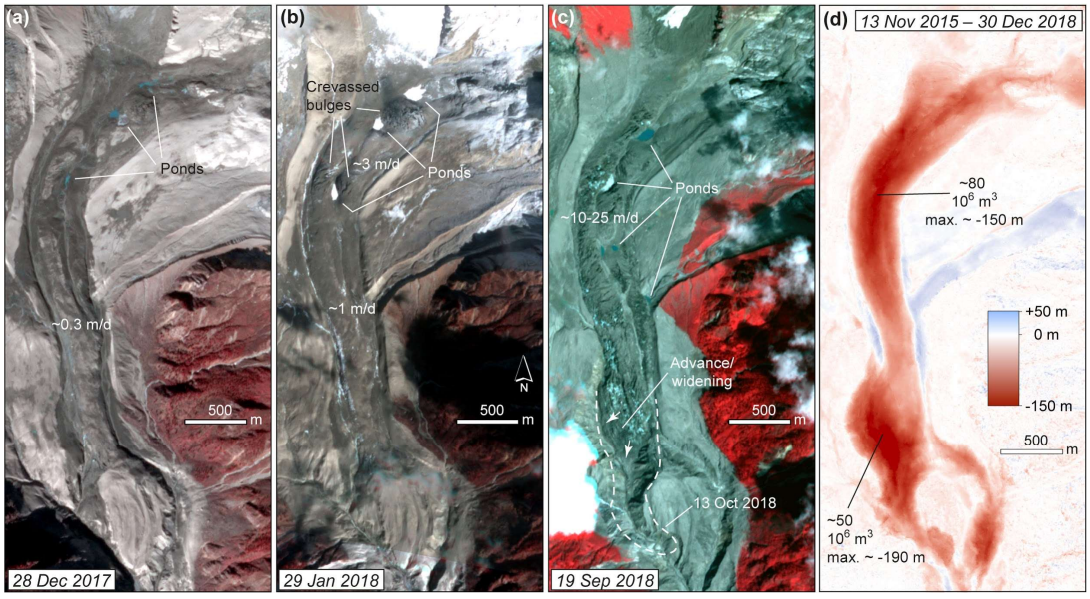

Figure 12: (a)-(c) Evolution of Sedongpu Glacier towards instability and detachment. Average surface velocities around the image dates are indicated. (Satellite images © Planet). Velocities and glacier position after 19 Sep 2018 (25 m/d) are derived from Sentinel-1 radar images. (d) Detail of elevation model differences between SPOT6 13 Nov 2015 and Pleiades 30 Dec 2018 tri-stereo data. Elevation losses amount up to 190 m, but the colour scale is saturated at -150 m.

3.6 Flat Creek, 2013, 2015 and 2016, Alaska

Flat Creek glacier, a small glacier in the north-eastern corner of Alaska's St. Elias mountains (Fig. 13), produced two large glacier detachments in 2013 and 2015. This region in Alaska is home to many surging glaciers (e.g., Harrison et al., 2015; Sevestre and Benn, 2015; Kochtitzky et al., 2019), and a glacier in a valley adjacent to Flat Creek surged between 2012 and 2016. Located in the rain shadow of the St. Elias range, the area receives on average about 350 mm of precipitation annually (2008 – 2018). A mean annual air temperature of -14°C at the former terminus of Flat Creek glacier, ground temperature measurements, and electrical resistivity tomography surveys strongly suggest that the headwall is underlain by continuous permafrost (Jacquemart et al., 2020).

On 5 August 2013, the lower 500 m of the glacier detached, releasing 6.8-11.2 10^6 m^3 of ice and lithic material. On 31 July 2015, most of the remaining glacier ice (up to the drainage divide) detached, evacuating an additional 17.6-20.1 10^6 m^3 (Jacquemart et al., 2020). Both events produced runouts of over 11 km (angle of reach 6-7°), deposited vast amounts of lithic

https://doi.org/10.5194/tc-2020-243
Preprint. Discussion started: 22 October 2020

material, and buried several km^2 of old growth forest (400+ years old). The large amount of fine-grained sediment found in the deposits suggests that the failures occurred within the glacier bed rather than at the ice-bed interface. The detachment slope was determined to be 21°.

A remarkable feature of Flat Creek glacier was a ~70 m tall bulge upstream of a stagnant, crevasse-free tongue. A similar bulge on Trapridge glacier, a polythermal surge-type glacier 80 km south-east of Flat Creek, was shown to have formed because a cold-ice tongue buttressed temperate ice upstream (Clarke and Blake, 1991). Based on the low annual air temperature and the presence of continuous permafrost, Jacquemart et al. (2020) concluded that the bulge on Flat Creek glacier was also the consequence of a polythermal regime. Measurements of the bulge position in satellite images suggest that the bulge advanced between 2011 and 2013, likely increasing driving stresses locally.

The 2013 and 2015 detachments both occurred at the peak of their respective melt seasons. Using a degree-day model, Jacquemart et al. (2020) found that the water availability during the exceptionally warm summer of 2013 was primarily melt driven and up to 4.8 standard deviations (σ) above the long term mean (1979–2015). No detachments were detected in 2014, when water availability was below average (-0.5 σ). Water availability was again higher in 2015 (+ 1 σ), when the second detachment occurred.

In 2016, a third glacier detachment released from a much steeper glacier (~30°) in the same cirque (not described in Jacquemart et al. (2020) but mentioned in Jacquemart and Loso (2019)). We differenced a 13 March 2016 Arctic DEM and a structure-from-motion DEM from a 2019 aerial survey and estimate the volume of this detachment to be 4.7 ± 0.18 10^6 m^3. Its causes have not been investigated, but the moving mass of ice was caught on video by rangers on a coincidental overflight. The speed of the observed mass flow was about three times slower than that of the 2013 and 2015 events. Nevertheless, the churning mass of ice blocks (termed a “slush-alanche” by Jacquemart and Loso (2019)) provides a sense of what the much larger flows may have looked like.

https://doi.org/10.5194/tc-2020-243
Preprint. Discussion started: 22 October 2020

The Cryosphere Discussions
Open Access
EGU

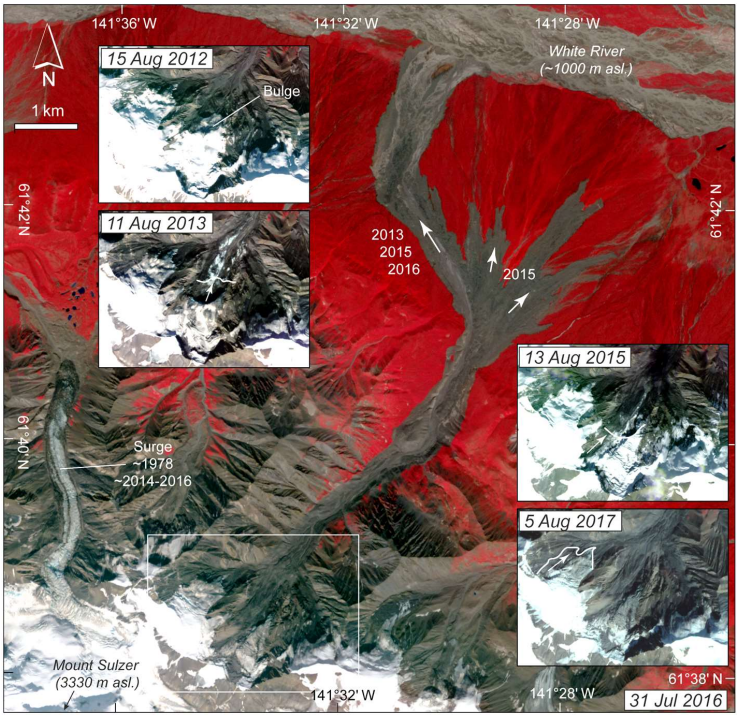

556 **Figure 13: Overview of the three detachments and ice-rock avalanches from Flat Creek Glacier, Alaska, since 2012. On the 15 Aug 2012 inset, a bulge is visible on the lower part of the glacier. On the 11 Aug 2013 inset, the glacier part** 558 **that detached on 5 Aug 2013 is indicated together with the front position before the event (white line). On the 13 Aug 2015 inset, the detachment of 31 Jul 2015 and the front position before it are indicated. On the 5 Aug 2017 inset, the** 560 **area of the 10 Aug 2016 detachment is shown. All images © Planet (Dove and RapidEye satellites). (For more images and front positions see Jacquemart et al. (2020)).**

562

3.7 Aparejo, 1980, Chilean Andes

564 On 1 March 1980, $7 \cdot 10^6$ m^3 (85% of its total volume) sheared off the debris-covered Aparejo Glacier in the Chilean Andes, mobilizing the detached mass 3.7 km down-valley with an estimated speed of 110 km/h (Ugalde et al., 2015; Ugalde, 2016; 566 Ugalde et al., 2017) (Fig. 14). The slide deposit covered an area of 0.55 km^2 with ice and rock debris piled up to 17 m thick. The volume of the deposit was estimated at 8.1 10^6 m^3 (Marangunic, 1980). Five mountaineers witnessed the event and noted

https://doi.org/10.5194/tc-2020-243
Preprint. Discussion started: 22 October 2020

several supraglacial ponds and 2-3 cm of wet snow on the surface of the glacier (Marangunic, 1980). These observations suggest that the triggering mechanism of the glacier detachment likely involved an extreme reduction of the basal drag due to high water saturation of the glacier bed. Aparejo glacier appears to sit on a glacier bed composed primarily of weak subglacial till , and the slope on the lower two thirds of the glacier averages 7°. Snowmelt infiltration and warm precipitation due to a sudden increase of the zero-degree isotherm elevation could have provided the main source of infiltrated water, leading to enhanced water pressure at the glacier bed. During a field inspection on 12 March 1980, Marangunic (1980) found that the nearby debris-covered glacier to the east, glacier no 51 according to the Chilean glacier inventory at the time (Fig. 14), also showed significant signs of surge-like instability, such as a heavily crevassed front and patches of freshly exposed ice along its entire length. The prominent terminal moraine of this glacier may have contained its detachment, though.

The Aparejo glacier is situated in a region of complex geology with a number of weak rock formations, including sandstones and fine-grained conglomerate in the immediate vicinity of the glacier (Ugalde, 2016). Ugalde (2016) sampled the grain size distribution of the remains of the lower ice-rock avalanche deposits and did not find them to contain more fines than a typical moraine, but notes that spatial variability was high and that the 35 years since the detachment may have depleted the deposits of fine particles. In the former avalanche path, modern satellite images show streamlined striations similar to those reported from several other detachments in this contribution. Remarkably, similar striations are also visible in Hycon airphotos from 1956. Interestingly, the geomorphology of the deposit area is similar between the 1956 airphotos and the post 1980-event high-resolution satellite images. One possible interpretation of this is that large mass flows had already originated from the Aparejo cirque at earlier times. A detailed field investigation would be required to determine whether the striations consist of glacial flutes formed under a previous glacier extent or stem from a catastrophic detachment.

In 2015, the glacier had around 15% of its pre-detachment volume, covering much of the original area, and with a surface slope of around 20° (Ugalde, 2016). The current glacier terminus lies at around 3400 m a.s.l., slightly below the lower regional limit of discontinuous permafrost, estimated by Brenning (2005) to be at around 3500 m a.s.l. Consistent with regional glacier mass balance trends (Falaschi et al., 2018b; Braun et al., 2019; Dussaillant et al., 2019), decreasing ice thicknesses have been identified on the lower and middle section of the Aparejo glacier (Ugalde et al., 2017), pointing to the glacier shrinking under current climate conditions.

https://doi.org/10.5194/tc-2020-243
Preprint. Discussion started: 22 October 2020

The Cryosphere
Discussions
Open Access
EGU

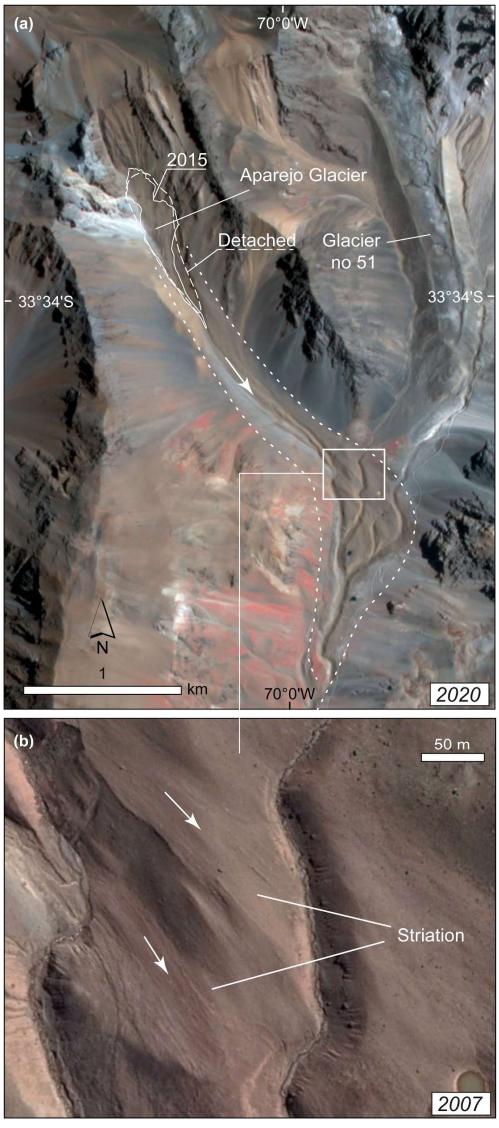

Figure 14: Aparejo Glacier, Chilean Andes. (a) Satellite image (© Planet) of 27 Jan 2020 with the outlines of the detached glacier as solid line, and the outlines of the 1980 detachment and runout roughly indicated as dashed lines (outlines after Marangunic, 1980; Ugalde, 2016; Ugalde et al., 2017). (b) Detail of avalanche path (rectangle in (a)) with streamlined ground striations. Satellite image: © Google Earth and CNES/Airbus, 29 Feb 2016.

https://doi.org/10.5194/tc-2020-243
Preprint. Discussion started: 22 October 2020

The Cryosphere Discussions
Open Access
EGU

598

3.8 Leñas, 2007, Argentinean Andes

600 The 4 10^6 m^3 detachment of Leñas Glacier between 5 and 14 March 2007 was discovered only recently, since it happened in a very remote region and had no down-stream impacts. Meanwhile, the case is described in detail by Falaschi et al. (2019).
602 The detached lower glacier section had a surface slope of around 15-16°. The glacier tongue at around 3450 m a.s.l. is suggested to lie within the zone of discontinuous permafrost in the region. The bed characteristics of the glacier are not known, but large
604 amounts of fine sediments were found over the run-out area of the event. A number of glacier surges are documented in the wider region but not for Leñas Glacier itself (Falaschi et al., 2018a, 2019). At the location of the later head scarp of the
606 detachment, pronounced transverse crevasses are visible in airphotos from 1970 and in a satellite image from a few weeks before the event (SPOT5). It is hard to determine, however, if these crevasses could have been signs of abnormal glacier
608 behaviour, or rather a pre-existing feature that then naturally formed the upper failure scarp. Transverse undulations of the glacier surface as indicated in the 2000 SRTM DEM, and a slight increase of surface gradients at the location of the crevasse
610 zone favour the latter scenario.

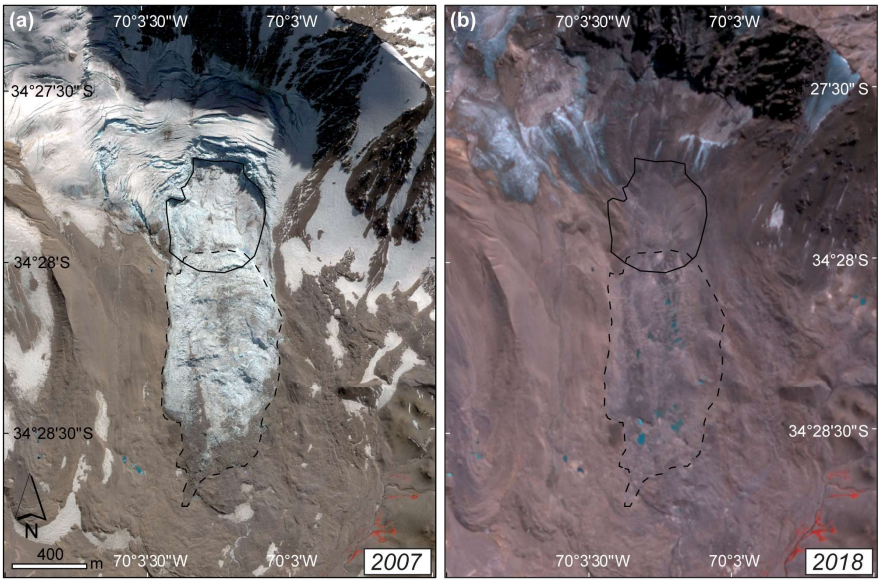

612 **Figure 15: (a) Quickbird satellite image of 19 Apr 2007 over Leñas Glacier, Argentinian Andes, a few days after detachment (© Maxar). (b) Planet image of 28 Mar 2018. Bold lines in both panels indicate the detached glacier part,**
614 **dashed lines the outlines of the avalanche deposits. (© Planet).**

https://doi.org/10.5194/tc-2020-243
Preprint. Discussion started: 22 October 2020

3.9 Tinguiririca, 1994 and 2007, Chilean Andes

3.9.1 The 1994, 2007 and a possible 1962 event

A detachment from a glacier on the southern flank of the Tinguiririca Volcano (Fig. 16) happened between 27 June (Landsat 5 TM) and 6 July 1994 (Landsat 5 TM). For the event, we estimate a detached glacier area of 0.2 km^2. Using glacier thickness estimates derived for the 2007 case (described below), we estimate a detachment volume of roughly 4–5 10^6 m^3. The climatic conditions between 1994 and 2007 were obviously favourable enough (i.e. little negative or even balanced regional glacier mass balances; Masiokas et al, 2016; Dussaillant et al. 2019) for the glacier to recover to its pre-detachment geometry.

At the same location, a glacier area of 0.46 km^2 detached between 7 January (Landsat ETM+ image without collapse) and 14 January 2007 (Landsat ETM+ with collapse), producing an ice/debris avalanche of 10–14 10^6 m^3 volume (Schneider et al., 2011; Iribarren Anacona et al., 2015; Figs. 16, 17). We estimate that the detached glacier had a surface slope of around 20°. Before the 2007 detachment, the glacier's lowest elevation was at about 3500 m a.s.l., roughly at the lower regional limit of discontinuous permafrost (Brenning, 2005). The volcanic nature of Tinguiririca should be associated with weak rocks and sediments. There are fumarolic fields and hot springs within a few km of the detached glacier (Pavez et al., 2016), and an inactive volcanic crater lies just a few hundred metres to the west of the detached glacier. In very high-resolution satellite images of 2007 and later (GoogleEarth, BingMaps), clear signs of hydrologic activity are visible in the upper part of the detachment area: freshly eroded channels, wet looking areas, and deposits from small debris flows – all perhaps signs of geothermally-enhanced melt of snow and ice (Fig. 17). In the path of the ice-rock avalanche we find streamlined striations similar to those found in the Kolka, Rasht 2019, and Aparejo avalanche paths (Fig. 17). As of late 2019, the glacier has not recovered from its 2007 detachment and there are only a few small snow (or ice?) fields visible at its location. Elevation differences between 2000 (SRTM DEM, before detachment), 2007–2010 (ALOS PRISM, after detachment), and 2010–2015 (TanDEM-X; both the ALOS PRISM and TanDEM-X DEMs are multi-year composites and therefore their date range is given) suggest that the detached glacier had average and maximum thickness of 21–28 m and 50 m, respectively. Combined with the detached glacier area of about 0.5 km^2 we estimate a detachment volume of roughly 10.5–14 10^6 m^3 , which is in good agreement with Iribarren Anacona et al. (2015). The Tinguiririca case illustrates how glacier removal by the 1994 detachment was largely reversible as the glacier built up again to failure conditions under the climate at that time, whereas the 2007 glacier removal seems irreversible under current climate and associated negative glacier mass balances in the region (Falaschi et al., 2018b; Braun et al., 2019; Dussaillant et al., 2019).

In airphotos from 1962 and Corona-series reconnaissance-satellite images from 1967 we notice striations in the valley similar to the ones visible after the 1994 and 2007 events, and other cases described in this contribution. Over the glacier, the 1962 airphotos clearly show that a glacier detachment similar to the 1994 event must have occurred not long (weeks, months or a

https://doi.org/10.5194/tc-2020-243
Preprint. Discussion started: 22 October 2020

few years?) before the image was taken. Stripes of debris or ice remains after the avalanche are still well preserved in the 1962 images over the glacier (Fig. 17d). (The associated terrain sections are under snow cover in the 1967 Corona images).

3.9.2 A potential large pre-1970s detachment of the neighbouring glacier

In the neighbouring valley to the east (Fig. 18) we note geomorphological traces that could be investigated further with regard to their origin from volcanic mass movements, earlier glacier stages, glacier surging, or more glacier-detachment like events. In the lower part of this potential event path we find striations, similar to the ones from the Tinguiririca, Aparejo and other avalanches of this study, largely unchanged since the first available Corona-series reconnaissance-satellite images in 1967 (Fig. 18c), and airphotos from 1962. Only detailed field work would be able to rule out the possibility that this striations consist of glacial flutes or small lateral moraines formed during a previous glacier extent, or were produced by a glacier surge. It should also be investigated whether such striations can remain largely intact after having been overrun by an ice-rock avalanche or if it is an indicator of the most recent event (see also Aparejo, where similar questions turned up).

In the upper part of this valley, or in the potential event source area, we observe two noticeable changes over time. First, the tongue of this unnamed glacier (RGI60-17.01112, GLIMS ID: G289692E34781S) was much smaller in 1962 airphotos than it is in 2020. Its advance of roughly 1.5 km since 1962, most of which occurred between 1975 and 1986 (Landsat), is in stark contrast to the pronounced shrinkage of the other glaciers in the area (Fig. 16 and 18). Indeed, differencing a DEM, which we produced from 1962 stereo-airphotos, from the SRTM or TanDEM-X DEMs confirms elevation gains on the glacier tongue of up to 120 m between 1962–2000 (SRTM), or up to 150 m between 1962 and 2010-2015 (TanDEM-X; Fig. 18c). This development could point to the recovery of the glacier tongue after a removal some time before 1962. The volume gain of the glacier tongue between 1962 and 2000 is around 70 10^6 m^3, or 100 10^6 m^3 between1962 and 2015.

Second, we detected an elevation decrease of the glacier forefield of around 10–15 m between 1962 and 2000, which could point to the deflation of debris-covered ground ice, deposited by a possible surge or glacier detachment (Fig. 18c). Third, a comparison of the 1962 airphotos to contemporary images revealed a heavily bulged glacier surface between 3900 m a.s.l. and 4650 m a.s.l. (Fig. 18a,b). Visually, this bulging is similar to the bulge found on Flat Creek Glacier prior to its 2013 detachment (section 3.6). The slope of the glacier tongue is around 8-10°, and around 35° for the steep upper part. The bulging upper part of the glacier is far above the regional permafrost limit so that polythermal ice conditions might well be found in parts of it.

We also examined a 1955 Hycon aerial photo (no stereo data to produce a DEM available to us), but visual interpretations from it remain inconclusive. Under illumination conditions that are very different from those of the 1962 images, the headwall glacierisation and the tongue seem larger in 1955 than in 1962, resembling rather its shape and extent of the 1980s. Below the position of the current (2020) glacier terminus, there seem to be dead-ice remains visible in the 1955 images. These are also visible in the 1962 images, though shrinked. It remains thus to be clarified at this point to which extent the features observed

https://doi.org/10.5194/tc-2020-243
Preprint. Discussion started: 22 October 2020

676 can be explained by a surge, or series of surges of the glacier before 1955, or between 1955 and 1962, or by a detachment-like event.

678

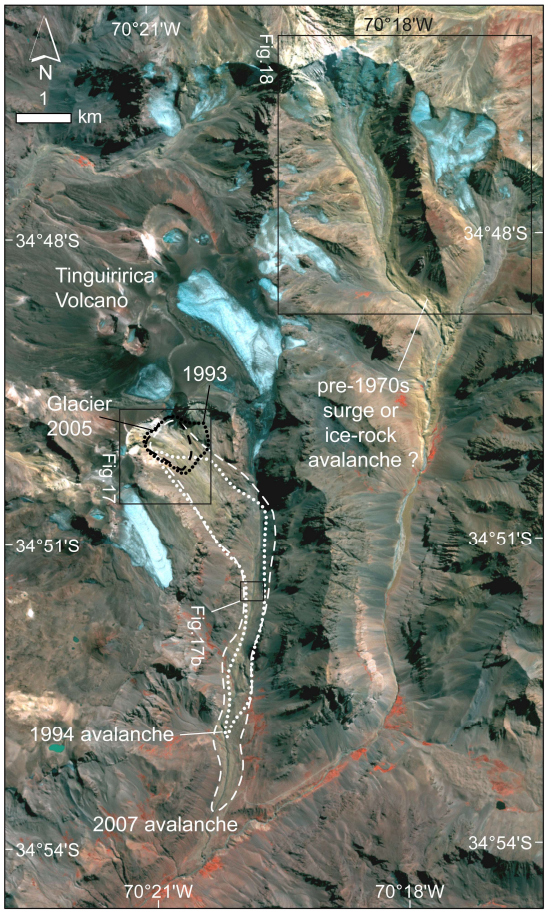

680 **Figure 16: Tinguiririca Volcano, Chilean Andes. Outlines of the 1994 and 2007 ice-rock avalanches, and the 1993 and 2005 area of the detached glacier as dotted or dashed lines, respectively. These outlines have been digitised for this** 682 **study but were found to agree well with the ones in Iribarren Anacona et al. (2015). Satellite image: Sentinel-2 (EU Copernicus), 14 Mar 2020.**

https://doi.org/10.5194/tc-2020-243
Preprint. Discussion started: 22 October 2020

The Cryosphere
Discussions
Open Access
EGU

684

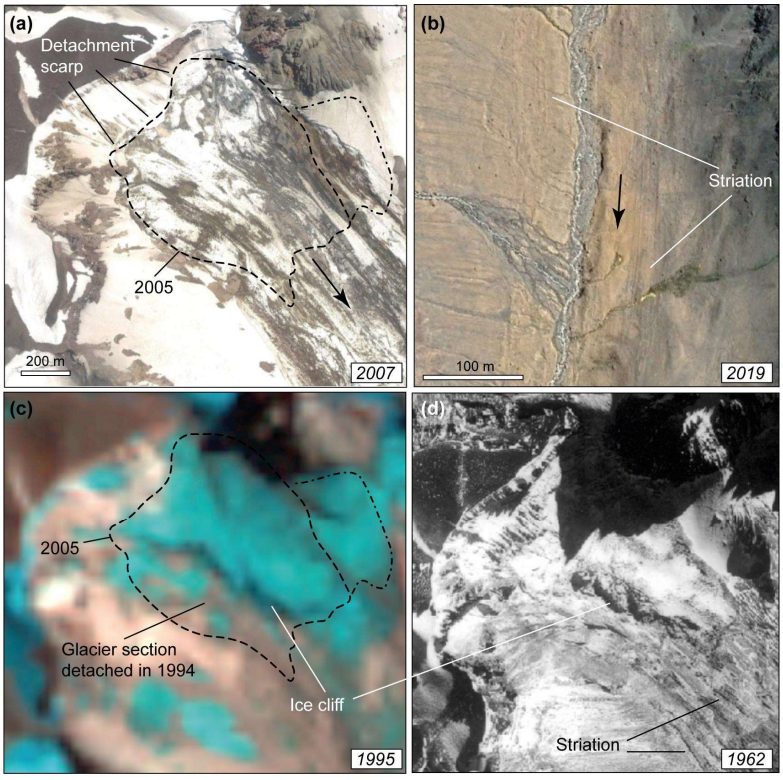

686

Figure 17: (a) Glacier detachment area at Tinguiririca Volcano on 24 Jan 2007 (satellite image: © Google Earth and
688 **Maxar). Glacier outlines from 26 Feb 2005 Landsat data (latest snow-free image before 2007 detachment) indicated by dashed line. From the 30-m resolution Landsat data it is unclear whether the dash-dotted ice section was connected to**
690 **the main glacier. (b) Striations left by the 2007 ice-rock avalanche (30 Jan 2019; © Google Earth and CNES/Airbus). (c) A Landsat image of 19 Mar 1995 (first snow-free image after 1994 detachment) shows that the southern part of the**
692 **glacier detached in the 1994 event. Glacier outlines of 2005 dashed as in (a). (d) The glacier on an aerial image of 8 Apr 1962 (© National Geographical Institute of Argentina). Clearly, a glacier section similar to the 1994 event has detached**
694 **not long before the image date, leaving also a similar ice cliff. Striations or streamlined features of debris/ice remains from the resulting avalanche are still well visible.**

https://doi.org/10.5194/tc-2020-243
Preprint. Discussion started: 22 October 2020

696

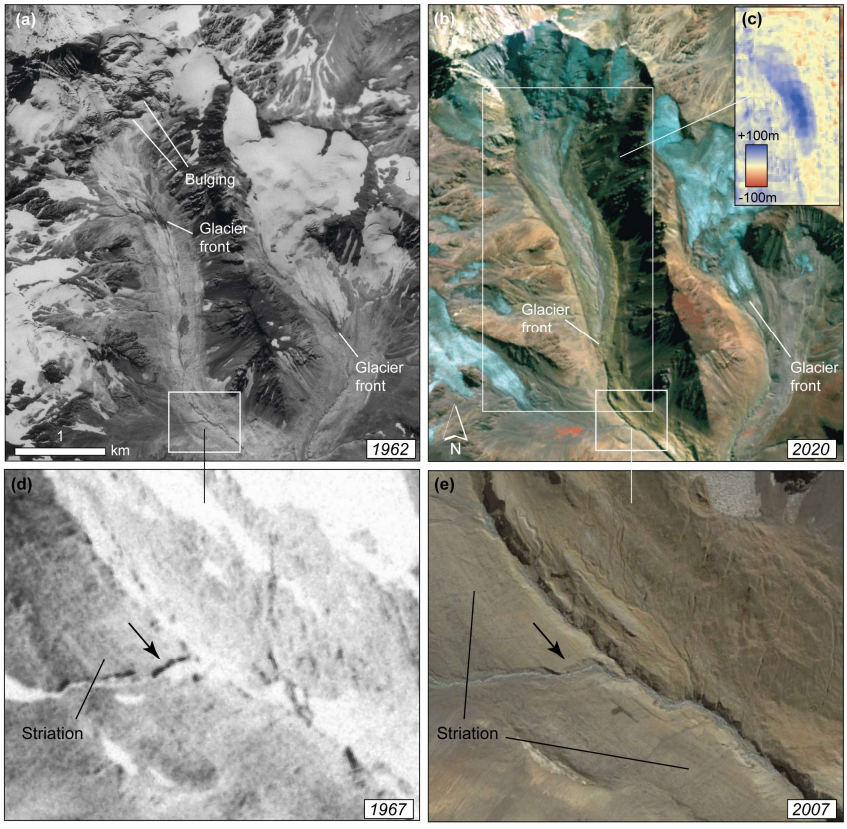

698 **Figure 18: Glacier valley with potential former surge or glacier detachment, east of Tinguiririca Volcano. See Fig. 16**
for location. (a) Orthoprojected airphoto of 8 Apr 1962 (© National Geographical Institute of Argentina). (b) EU
700 **Copernicus Sentinel-2 image of 14 Mar 2020, showing an advance of 1.5 km relative to 1962, in contrast the other**
retreating glaciers in the area. (c) Elevation differences between DEMs from 1962 stereo airphotos and the 2000 SRTM
702 **show gains over the glacier tongue of up to 120 m, and losses of around 10-15 m in the forefield. (d) Corona satellite**
image of 23 Feb 1967 with striations. (e) Satellite image of 19 Mar 2007 (© Google Earth and Maxar). (a) and (b), and
704 **(d) and (e) show the same terrain section each. Locations of (c), (d) and (e) indicated as white rectangles in (a) and (b).**

https://doi.org/10.5194/tc-2020-243
Preprint. Discussion started: 22 October 2020

4 Discussion

4.1 Commonalities and differences

The most apparent similarities among the detachments compiled in this contribution (Tab. 1) are their geographic proximity to surge-type glaciers – in some cases the detached glaciers themselves exhibited surging or surge-like behaviour – as well as the existence of weak bedrock and/or fine sediments around and likely at the base of the glaciers (Tab. 2). Both commonalities suggest that the sudden detachments of low-angle glaciers discussed here could be seen as rare and extreme endmembers of the range (Quincey et al., 2015; Herreid and Truffer, 2016) of surge-type and surge-like glacier instabilities. The detachments could be a specific kind of glacier surge where the force balance cannot be achieved by a global control, typically by geometric adaptation, when basal friction is suddenly reduced. In combination with a low bed roughness and an absence of sufficient topographic support, the reduced amount of stress accommodated by basal resistance has nowhere to be transferred to and leads to an expanding force imbalance (Thogersen et al., 2019). This ultimately leads to a runaway acceleration and detachment. this is not quite the right terminology. The glacier is in force balance until failure occurs. This is a sudden transition.

In this context, we note that the surface slopes of the detached glaciers were between 9° and 21° (average 15.9°, standard deviation 3.6°), which is at the upper end for slopes of surge-type glaciers, yet surprisingly low for glaciers causing ice avalanches. The slope range of around 10–20° may be a necessary condition for glacier detachments, as these – for surge-type glaciers – comparably high slopes are large enough to increase the probability of exceeding a critical shear stress and thus allowing for sudden basal failure. At the same time, glaciers within the 10–20° slope range still have considerable thickness and thus volume, while higher slopes sustain thinner glaciers and much smaller volumes involved in a potential failure (Fig. 1c). Our very limited data base of detachment events suggests a transition between larger and smaller detachment volumes at roughly around 14° (Fig. 1c).

From a more mechanical point of view, low-angle glacier detachments can also be seen as part of the continuum between surges and ice break-offs from steep glaciers. Not least owing to their slope, glaciers have a range of possibilities to adapt to changes in their stress regimes (see Fig. 18). Flat glaciers can respond by adjusting their geometry, for instance through advance and surging. On very steep terrain, glaciers may not be able to adjust their geometry smoothly and ice breaks off. In contrast to the factors involved in typical ice break-offs from steep glaciers (see section 1), glacier detachments appear to have in common basal failure on soft beds. Therefore, low-angle glacier detachments combine the elements of both instability processes: the inability to rapidly adjust geometry in response to stress changes, similar to steep glaciers, and a surge-like process that propagates an initial instability through large parts of the glacier (Thogersen et al., 2019), allowing entire glacier tongues to be mobilized. The latter framework for low-angle glacier detachments and the above one of surge endmembers are not mutually exclusive but rather linked by the role of glacier slope, fine basal tills, and the surge-like propagation of instabilities.

https://doi.org/10.5194/tc-2020-243
Preprint. Discussion started: 22 October 2020


The Cryosphere Discussions
Open Access
EGU

The role of basal water pressure in the detachments is difficult to examine in detail, but most detachments could have involved severe reduction in friction due to high basal water pressure (likely at least for Kolka 2002, Aru, Flat Creek, Sedongpu, Aparejo). Ways to rapidly increase basal water pressure include: an increase in water input (e.g., large high-altitude rain events (Kääb et al., 2018) or increased surface snow/ice melt) into a subglacial drainage system not capable of adjusting fast enough; inefficiencies or blockages of this drainage system; or increased permeability of the glacier through enhanced crevassing (Dunse et al., 2015). Sudden weakening of the strength of subglacial till under high pore water pressure and over large parts of the glacier bed was shown to be a key process leading to the Aru detachments (Gilbert et al., 2018). Ongoing surge-like activity may enhance sensitivity to water input (Flowers et al., 2016).

In Figure 18 we attempt to summarize the main drivers of the glacier detachments described here. We define a detachment's *disposition* as the sum of long-term factors that might promote glacier detachments and refer to *triggers* to describe short-term factors that might suddenly tip the scale toward a catastrophic failure. Fundamentally, it seems that different combinations of dispositions and triggers are able to produce instability. Aside from the commonalities mentioned above, the observed detachments all present some unique conditions, many of which remain shrouded in uncertainty. The observed failure conditions (Tab. 2) include ruptures during surge-like glacier instabilities (Kolka 1902, Aru, Amney Machen, Sedongpu; unclear for Devdorak), or increase of driving stress due to thickening caused by snow accumulation (Aru) or rock-ice avalanches (Kolka 2002, Sedongpu?). Geothermal activity could have played a role at Tinguiririca and Kolka, but is unlikely for the other events. The thermal setting of the detached glaciers can play a role if permafrost around the glaciers potentially causes frozen margins or the glaciers exhibit a polythermal structure (Aru, Flat Creek, Tinguiririca?, Leñas?). However, other detachments happened under conditions very likely free of cold ice. Some of the detached glaciers seem to have been composed of a mixture of debris and ice (Amney Machen, Flat Creek; likely at least for Devdorak, Kolka, Sedongpu). Such mixtures can be profoundly weaker than clean glacier ice, particularly at temperatures close to the melting point (Moore, 2014), but it is unclear at this point whether and how these mixtures and their weakness may have contributed to the detachments. In contrast, the ice of the Aru glaciers clearly consisted of rather clean ice. Failure circumstances are particularly unclear to us for Aparejo and Leñas.

The angles of reach of the ice-rock avalanches associated with glacier detachments (Fahrböschung between about 5° and 10°), both absolutely and relative to their volume, are lower or at the lower end of those observed for other types of ice-rock avalanches (Fig. 1a, b). The particularly high ice content of glacier detachments might reduce friction of the mass movements through liquefaction (Schneider et al., 2011), promoting the long runouts. Remarkably, many (all?) detached glaciers appear to have sat on particularly fine-grained glacier beds. The large amounts of soft sediments under the glaciers, combined with the presence of (unusually?) large amounts of basal water at the time of detachments, may have decreased the friction angle by lubrication and allowed the detachments to accelerate particularly fast on a basal slurry. In addition, smooth u-shaped glacial valleys might favour low angles of reach by channelizing the mass flows, reducing energy dissipation, and presenting few topographic obstacles along the path (Schneider et al., 2011).

the friction angle is a sediment property and independent of water pressure

https://doi.org/10.5194/tc-2020-243
Preprint. Discussion started: 22 October 2020

4.2 Influence of climate change

and also for some steep glacier failures

Inevitably, questions arise as to what extent climate change could be a driving factor of glacier detachments. Some cases investigated here suggest situations where repeated detachments could be part of a cycle from reservoir refilling up to occasional threshold exceedance, similar to what is found for glacier surges (Benn et al., 2019; Amney Machen, Tinguiririca, Devdorak, Kolka, Rasht?). But several cases of this study also illustrate developments where climate change can cause transient conditions that lead to failure. The twin Aru detachments, which detached within just two months of each other, strongly point to a common meteorological trigger as the only possible external driver able to synchronize the two events. A number of dispositions and triggers listed in Fig. 18 may be impacted by climatic changes and may bring a glacier closer to failure.

or prevent future events

Repeated detachments of the same glacier, or detachments connected to surge-like behaviour, require that the climate conditions and associated glacier mass balances enable reservoir recovery or built-up of accumulation areas (Devdorak, Aru, Amney Machen, Kolka 1902). Climate change might shift glaciers out of the envelope of conditions that are favourable for surging, or shift them into it (Hock et al., 2019). Whereas glacier rebuilding seems to be underway at Kolka and Aru, it is open for Sedongpu, and unlikely for Tinguirica. The glacier's potential to regain a substantial size is critically linked to the potential for repeated detachment events, and thus important for hazard management.

The enhanced rock-ice avalanching onto Kolka Glacier in 2002, possibly responsible for its detachment, or the 2017 Gyala Peri rock avalanche over the Sedongpu Glacier, are likely a reflection of climate change impact on polythermal, glacierised rock walls, where the reduction of ice cover and permafrost thaw increases the rock and ice fall frequency (Fischer et al., 2013). Indeed, summers were exceptionally warm and glacier mass balances negative in the Caucasus Mountains, which host Kolka Glacier, over 1998–2001 (Zemp et al., 2019). Glacier shrinkage due to negative mass balance (Larsen et al., 2015; Treichler et al., 2019; Zemp et al., 2019) has exposed large parts of the – at earlier times mostly ice-covered – headwalls of Flat Creek, Amney Machen, Leñas, and likely Petra Pervogo/Rasht. This exposes bedrock to erosion making it available for mass flows and incorporation in and underneath the glaciers, a process that is particularly important for soft rock lithologies. The partial loss of glacier cover may also interrupt existing patterns of stress transfer and cause new temporary stress concentrations (see also Fig. 18) that may exceed stability thresholds in certain locations. Some glacier detachments could thus be connected to the transient development of headwall glacier loss.

Climate change increases the amount of meltwater and transitions from snowfall to rainfall, and may thus favour development of instabilities, at least for the polythermal glaciers (Aru and Flat Creek) where such amount of meltwater is unusual at the scale of the last century. The relative increase of meltwater can be particularly significant for cold/dry climate glaciers.

4.3 Hazard management

From a more applied hazard management perspective, sudden massive glacier detachments pose a high magnitude/low-frequency problem, and their low probability/high consequence nature makes them hard to incorporate in hazard management

https://doi.org/10.5194/tc-2020-243
Preprint. Discussion started: 22 October 2020

and planning. The particularly low friction coefficients (H/L) involved in the detachments enable them to travel over low slopes (where other types of ice-rock avalanches would stall) and to cover large distances. The detachment events seem very rare, but their large volumes, fast evolution, and the exceptionally long reaches and high speeds hold the potential for severe impacts even far away from the source. Our compilation of all (so far) known cases shows that low-angle glacier detachments might have, though rare, more frequently occurred than thought. The differences between the events suggest that there is no straightforward way to predict where they might occur, but the following list of the most common conditions might support a more systematic assessment. Events happened at places

(i) with abundant weak bedrocks/fine sediments,
(ii) where glacier surface slope is between about 10° and 20°,
(iii) where surge-like glacier instabilities are observed in the region, or for the detached glacier itself, and
(iv) where similar events or other violent ice-rock mass flows have happened before (based on direct observation or a geomorphological imprint).

This set of very rough qualitative criteria might allow a first-order assessment of whether glacier detachments are possible in any given region. It is crucial to be aware of, however, that these criteria and their interplay are likely transient so that in particular criterion (iv) can be misleading. For several of the events we find streamlined debris features or striations in the avalanche paths, but highlight that more research is necessary to correctly interpret these signatures and differentiate them from glacial flutes, small moraines, and other longitudinal glacial and geomorphodynamic features. Particularly important for hazard management is – yet again – the conclusion that climate change is able to shift hazard zones beyond historical precedence, so that also so far unaffected areas might suddenly be susceptible (Hock et al., 2019).

Systematic monitoring turns out to be one of the most feasible responses to changes in hazard conditions, and the increasing temporal and spatial resolution, and improving availability of satellite imagery, is particularly helpful for glacier detachment assessment. For several of the cases in this contribution, abnormal glacier crevassing and accelerating precursory speeds were visible days to weeks before failure (Kolka 2002, Rasht, Aru, Sedongpu, Flat Creek?), but the significance of such a development was realized for the second Aru detachment only due to its spatial and temporal proximity to the first Aru detachment. On the other hand, abnormal crevassing does not necessarily indicate an impending detachment, see Rasht 2007 or Leinss et al. (2019), where the glacier geometry has likely stabilized a detaching ice mass. Overall, predicting glacier detachments can likely only be achieved by strong efforts in detailed remote-sensing based monitoring and, if feasible, by ground-based measurements, which contribute to an improved understanding of conditions and relevant processes, past events, glacier velocities and slope deformations, glacier bed geology and lithology, surge behaviour and dynamics, and short-term and long-term temperature and precipitation records (Kääb et al. 2018).

https://doi.org/10.5194/tc-2020-243
Preprint. Discussion started: 22 October 2020

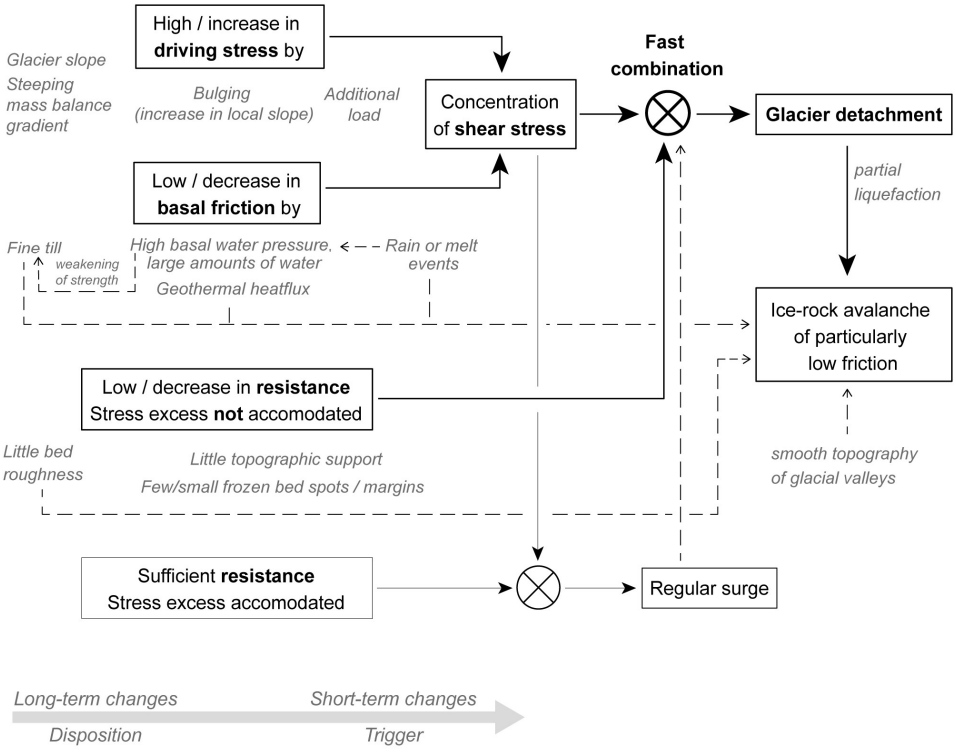

Figure 18: Schematic on which conditions and changes to a low-angle mountain glacier can in combination lead to the spatio-temporal interference of particularly high and concentrated shear stresses and low resistance, eventually exceeding stability thresholds and causing detachment. The failure conditions can change at a range of time scales, so that detachment is the result of a highly transient and rare interplay of factors. It is key that the low basal friction and high driving stresses, the resulting concentration of high shear stresses, and the lack of sufficient resistance develop fastly, or are combined fastly, preventing the glacier to adjust to changing forces in a steady way. Several of the factors potentially involved in the detachment are subsequently also able to strongly reduce basal friction of the resulting ice-rock avalanche and lead thus to particularly low angles of reach. Boxes in the figure indicate main physical conditions, grey italic text indicates different actual processes that can fulfil these conditions, sorted from long-term (left) to short-term (right) variability.

rapidly

5 Conclusions

In this contribution we describe around a dozen ice-rock avalanche events that we characterize as sudden large-volume detachments of low-angle glaciers. Overall, these events seem to be more frequent than previously thought. The detached volumes ranged from a few up to more than 100 10^6 m^3. We described one new event in the same size-class as the 2002 Kolka

https://doi.org/10.5194/tc-2020-243
Preprint. Discussion started: 22 October 2020

and the 2016 Aru glacier detachments (Sedongpu 2018) and as a side-result quantified one of the larger high-mountain rock avalanches of recent decades (Gyala Peri 2017).

Despite the relatively low number of low-angle glacier detachments and their site-specific variations that leave considerable uncertainties, we were able to identify a set of conditions and evolutions likely involved in these glacier failures. We consider this an important step, given that a few years ago the possibility for low-angle mountain glaciers to detach and produce massive ice-rock avalanches was hardly known. Interestingly, the fact that the spatio-temporal factor combinations leading to exceptionally low basal friction and very high shear stresses, and eventually to detachment, are different among the cases, suggests that there exists an exceptional but still fundamental possibility of low-angle glacier beds to fail catastrophically. Awareness of this fundamental potential for catastrophic basal instability expands our understanding of glacier flow.

Many of the glacier detachments show some relation to surge-type glacier movement, and could be seen as a rare and extreme endmember of this much more common glacier instability. Glacier detachments combine elements of surging, where the glacier adjusts its geometry to satisfy the force balance, with those of ice break-offs from steeper glaciers, where the glacier is not able to adjust in a steady way. The surface slopes of 9–21° of the detached glacier parts, though quite low for glaciers that produce ice avalanches, rank rather high in comparison with surge-type glacier tongues. Slopes in this range exert higher shear stresses than is typical for surge-type glaciers and favour thus the possibility of exceeding a critical stress level that then leads to sudden failure. At the same time, in comparison to glaciers in very steep terrain that tend to be thin, glaciers of 10–20° surface slope can build up thicker ice, which leads to the larger volumes typically involved in detachments.

Weak bedrock and/or the existence of soft and highly erodible sediments under the detached glaciers was identified for most of the observed glacier detachments, plausible for the ones we determined retroactively, and hints at till-strength weakening under high pore water pressure as a concrete failure process. There appear to be different trajectories into, or out of, the narrow envelope of potential failure conditions, not least driven by climatic changes. The fact that most collapses happened during local spring/summer suggests that a meltwater or high-altitude rain driven increase of basal pore water pressure can play an important role in triggering the events, whether directly or in some delayed form. Atmospheric warming enhances such hazard conditions. For some detachment sites, negative regional glacier mass balances can prevent detached glaciers from fully rebuilding and thus from detachments to repeat over time, at least at earlier volumes.

Detailed investigations of the events described in this study showed that a wide variety of dispositions and triggers can lead to a glacier detachment. This makes it challenging for practitioners working in high-mountain hazard management to anticipate and predict such events. From this practical standpoint, however, this study attempts to raise awareness about the – albeit low – possibility of sudden, large-volume detachments of low-angle glaciers at locations with

- particularly soft and erodible lithologies, and, likely related, the
- existence of surge-type glaciers and surge-like glacier evolution.

https://doi.org/10.5194/tc-2020-243
Preprint. Discussion started: 22 October 2020

878 - Repeated events or geomorphological imprints of potential earlier collapses or other violent ice-rock mass flows can be further investigated, but events can also happen without historical precedence through shifts in the array of failure
880 conditions.
- Several of the glaciers investigated here showed abnormal crevassing and enhanced precursory surface speeds in the
882 days to weeks before detachment.
- The surface slopes found in this study for the detached glaciers ranged between roughly 10° and 20°.

884 Due to the large amounts of snow and ice involved in glacier detachments, the high chance of lubrication and of liquefaction of glacier ice and subglacial sediments, and smooth geometries of glacial valleys, avalanche friction is typically greatly
886 reduced. This results in the particularly high mobility of the ice-rock avalanches resulting from low-angle glacier detachments and can lead to substantial damage far from the source. Between the large runout distances and the varying factors that can
888 impact a glacier's detachment probability, high-mountain hazard management will, after the first general assessment provided in this study, benefit from more detailed investigations of glacier detachments, the conditions that lead to them and the
890 mechanics that drive them.

892

https://doi.org/10.5194/tc-2020-243
Preprint. Discussion started: 22 October 2020

894 **Table 1: Parametres for the low-angle glacier detachments of this contribution. For repeat events the parameters given refer to the underlined year.**

Name of event	Region	Years	Lat, Lon	GLIMS,RGI IDs	Reach L (km)	Drop H (km)	Volume (10^6 m^3)	Glacier surface slope (°)	Section
Devdorak	Caucasus	1776, 1778, 1785, 1808, 1817, 1832, 2014	42.72°N, 44.55°E	G044517E42715N, RGI60-12.00840	10.5	3.2	15	17?	3.1
Kolka	Caucasus	~1835?,1902, 2002	42.73°N, 44.44°E	G044447E42733N, RGI60-12.00131	19	2.0	130	13	3.1
Rasht	Pamirs	2017	38.975N 70.850E	G070852E38974N, RGI60-13.18284; USSR 504	7.6	1.4	6	16	3.2
Rasht	Pamirs	2019	38.989° N 70.693° E	G070689E38981N, RGI60-13.20645; USSR 518	6.7	1,5	4.5	20	3.2
Aru 1	Western Tibet	Jul 2016	34.02° N, 82.250° E	G082249E34023N, RGI RGI60-13.51473, Chinese: CN5Z412C0011	8.2	0.8	68	12	3.3
Aru 2	Western Tibet	Sep 2016	34.00° N, 82.265° E	G082268E34005N, RGI60-13.51476, Chinese inv.: CN5Z412C0007	7.2	0.83	83	13	3.3
Amney Machen	Eastern Tibet	2004,2007, 2016,2017,2019	34.82°N 99.44°E	G099443E34824N, RGI60-13.23943, Chinese inv: CN5J352E0017,	5.2	1.0	27	15	3.4
Sedongpu	South-eastern Tibet	2018	29.80° N 94.92° E	G094940E29811N, RGI60-13.01391, Chinese inv.: SDP1	8	1.3	100	9	3.5
Flat Creek	Saint Elias Mts.	2013, 2015, 2016	61.50° N, 141.54° W	G218441E61638N, RGI60-01.17460	11	1.1	14	21	3.6
Aparejo	Chilean Andes	1980	33.56° S, 70.01° W	only World Glacier Inv. CL1M005D0049	3.7	0.8	7.2	20	3.7
Leñas	Argentinean Andes	2007	34.46° S 70.05° W	G289941E34459S, RGI60-17.01251	2	0.2	4.2	15	3.8
Tinguiririca	Chilean Andes	~1960,1994, 2007	34.83° S 70.35° W	only World Glacier Inv. CL1M00420016	7.9	1.4	12	20	3.9

https://doi.org/10.5194/tc-2020-243
Preprint. Discussion started: 22 October 2020

The Cryosphere Discussions
Open Access
EGU

896

Table 2: Possible indicators for and factors involved in low-angle glacier detachments.

Name of event	Earlier surges in the region?	Weak rocks, fine sediments ?	Glacier tongue within permafrost ?	Abnormal crevassing before failure?	Enhanced water input into glacier (melt, rain) ?	Repeat events known?	Signs of high water pressure ?	Signs of earlier mass flows?	Surge-like activity related to event?	Loading prior to event (snow, rock)?	Earlier surges same glacier ?	Bulging before event?
Kolka												
Devdorak												
Aru												
Sedongpu												
Rasht												
Amney Machen												
Flat Creek												
Tinguiririca												
Aparejo												
Leñas												

yes | uncertain yes | unknown | uncertain no | no

898

900

https://doi.org/10.5194/tc-2020-243
Preprint. Discussion started: 22 October 2020

Code availability

Not relevant

Data availability

Sentinel-1 and Sentinel-2 data are freely available from the ESA/EC Copernicus Sentinels Scientific Data Hub at https://scihub.copernicus.eu (Copernicus, 2020), Landsat satellite data, Corona satellite data, and SRTM-C DEMs from United States Geological Survey (USGS, 2020), SRTM-X and TanDEM-X DEMs from the German Aerospace Center (DLR, 2020), the ALOS World DEM from the Japan Aerospace Exploration Agency (JAXA, 2020), Chinese earthquake data from the China Earthquake Data Center. Planet data (Dove and RapidEye) are not openly available as Planet is a commercial company. However, scientific access schemes to these data exist (https://www.planet.com/markets/education-and-research/). Data from Maxar satellites (GeoEye, Ikonos, WorldView, Quickbird) and Airbus (Pléiades, Spot) are commercial, but in parts explorable from GoogleEarth and BingMaps.

Author contribution

A.K. wrote the text, did most new analyses and prepared the figures. M.J. wrote parts of the text, edited all text, and contributed comments and discussions. L.G. prepared the Sedongpu DEMs. All authors edited text and contributed with data, comments and discussions.

Competing interests

All authors declare that they have no competing interests.

Acknowledgements

This paper is an extended and updated version of the Louis Agassiz medal lecture by A.K. given at the European Geosciences Union General Assembly 2019.

The underlying work was funded by the ESA projects GlobPermafrost, Permafrost-cci, Glaciers_cci, and the ESA EarthExplorer10 Mission Advisory Group, and the European Research Council under the European Union's Seventh

https://doi.org/10.5194/tc-2020-243
Preprint. Discussion started: 22 October 2020

Framework Programme. We are grateful to the providers of free data for this study; European Space Agency (ESA) / European Commission (EC) Copernicus for Sentinel-2 data, USGS for Landsat, Corona, and SRTM data, DLR for SRTM and TanDEM-X data, and Planet for their cubesat data via Planet's Ambassadors Program. E.B. and S.G. acknowledge support from the French Space Agency (CNES) through TOSCA and DINAMIS programs. S.C. acknowledges support from Lomonosov Moscow State University on the theme “Mapping, modeling and risk assessment of dangerous natural processes”. D.P. and S.C. acknowledge the Russian Foundation for Basic Research (grant 18-05-00520). Paola Banegas from SEGEMAR Mendoza provided the 1962 aerial photos over Tinguririca.

Financial support

This work was funded by the ESA projects Permafrost_CCI (4000123681/18/I-NB), Glaciers_CCI (4000109873/14/I-NB, 4000127593/19/I-NS), and the ESA EarthExplorer10 Mission Advisory Group (4000127656/19/NL/FF/gp), by the European Research Council under the European Union’s Seventh Framework Programme (FP/2007-2013) / ERC grant agreement no. 320816, and the Russian Foundation for Basic Research (grant 18-05-00520)

https://doi.org/10.5194/tc-2020-243
Preprint. Discussion started: 22 October 2020

References

Alean, J.: Ice avalanche activity and mass balance of high-altitude hanging glaciers in the Swiss Alps, 6, 248-249, 1985.

Aristov, K. A., Petrakov, D. A., Kovalenko, N. V., Timonin, S. A., Kolchin, A. A., and Drobyshev, V. N.: Monitoring of Kolka Glacier in 2014–2017 by terrestrial stereophotogrammetry. Led i Sneg. Ice and Snow [In Russian], Led i Sneg (Ice and Snow), 59, 49–58, https://doi.org/10.15356/2076-6734-2019-1-49-58, 2019.

Asoyan, D. S., and Rototaeva, O. V. Devdoraki Glacier, Kazbek: history of studies of natural hazards in XIX and the beginning of XXI centuries. Led i Sneg. Ice and Snow, 56(2): 253-264, 2016. https://doi.org/10.15356/2076-6734-2016-2-253-264

Benn, D. I., Fowler, A. C., Hewitt, I., and Sevestre, H.: A general theory of glacier surges, J Glaciol, 65, 701-716, https://doi.org/PII S0022143019000625, 10.1017/jog.2019.62, 2019.

Braun, M. H., Malz, P., Sommer, C., Farias-Barahona, D., Sauter, T., Casassa, G., Soruco, A., Skvarca, P., and Seehaus, T. C.: Constraining glacier elevation and mass changes in South America, Nat Clim Change, 9, 130-+, https://doi.org/10.1038/s41558-018-0375-7, 2019.

Brenning, A.: Geomorphological, hydrological and climatic significance of rock glaciers in the Andes of Central Chile (33–35°S), 16, 231-240, https://doi.org/10.1002/ppp.528, 2005.

Brun, F., Berthier, E., Wagnon, P., Kääb, A., and Treichler, D.: A spatially resolved estimate of High Mountain Asia glacier mass balances from 2000 to 2016, Nature Geosci, 10, 668-673, https://doi.org/10.1038/ngeo2999, 2017.

Caplan-Auerbach, J., and Huggel, C.: Precursory seismicity associated with frequent, large ice avalanches on Iliamna volcano, Alaska, USA, J Glaciol, 53, 128-140, https://doi.org/Doi 10.3189/172756507781833866, 2007.

Chen, C., Zhang, L. M., Xiao, T., and He, J.: Barrier lake bursting and flood routing in the Yarlung Tsangpo Grand Canyon in October 2018, J Hydrol, 583, Artn 124603, https://doi.org/10.1016/j.jhydrol.2020.124603, 2020.

Chernomorets, S. S. New “Kazbek blockage” on 17 May 2014. Priroda, 7: 67-72 https://istina.msu.ru/download/6618200/1k5k5t:82mOHGauqEFijKJOHSXRsTVDIT8/ (in Russian), 2014.

Chernomorets, S., Savernyuk, E., Petrakov, D., Dokukin, M., Gotsiridze, G., Gavardashvili, G., Drobyshev, V., Tutubalina, O., Zaporozhchenko, E., Kamenev, N., Kamenev, V., Kääb, A., Kargel, J., and Huggel, C.: The Devdorak ice-rock avalanche and consequent debris flow from the slope of Mt. Kazbek (Caucasus, Georgia) in 2014, EGU General Assembly Conference Abstracts, April 01, 2016, 2016.

Chernomorets, S. S., Tutubalina, O. V., Seinova, I. B., Petrakov, D. A., Nosov, K. N., and Zaporozhchenko, E. V.: Glacier and debris flow disasters around Mt. Kazbek, Russia/Georgia, in: Debris-Flow Hazards Mitigation: Mechanics, Prediction, and Assessment, edited by: Chen, C. L., and Major, J. J., Millpress, Netherlands, 2007.

Clarke, G. K. C., Collins, S. G., and Thompson, D. E.: Flow, thermal structure, and subglacial conditions of a surge-type glacier, Can J Earth Sci, 21, 232-240, https://doi.org/10.1139/e84-024, 1984.

Clarke, G. K. C., and Blake, E. W.: Geometric and thermal evolution of a surge-type glacier in its quiescent state - Trapridge Glacier, Yukon-Territory, Canada, 1969-89, J Glaciol, 37, 158-169, 1991.

Copernicus Open Access Hub, Copernicus programme, European Commission and European Space Agency, available at: https://scihub.copernicus.eu, last access: 17 October 2019. , 2019.

Crandell, D. R., and Fahnestock, R. K.: Rockfalls and avalanches from little Tahoma Peak on Mount Rainier, Washington, U.S. Geol. Surv. Bull., 1221-A, A1-A30, 1965.

https://doi.org/10.5194/tc-2020-243
Preprint. Discussion started: 22 October 2020

Dokukin, M. D., Bekkiev, M. Y., Kalov, R. H., Savernyuk, E. A., and Chernomorets, S. S.: Signs of catastrophic glacier detachments (Analysis of multitemporal space information) (In Russian), in: Dangerous natural and technogenic processes in mountain regions: models, systems and technologies, Moscow, 522-528, 2019.

Dokukin, M. D., Savernyuk, E. A., and Chernomorets, S. S. Rock Avalanches in the Alpine Zone of the Caucasus in the 21 Century. Priroda, 7: 52-62, 2015. (in Russian).

Dokukin, M. D., Bekkiev, M. Yu., Kalov, R. Kh., Chernomorets, S. S., and Savernyuk, E. A. Activation of rock avalanches in the Central Caucasus and their impact on the dynamics of glaciers and debris flows. – Led i Sneg. Ice and Snow, 60(3): 361-378, 2020.

Drobushev V.N., Torchinov H-M.Z., Tutubalina O.V., and Hubaev H.M. Main topographical data and kinematics of the Devdorakskiy collapse on May 17, 2014. Vestnik of the Vladikavkaz Scientific Centre, 4: 30-41, (in Russian), 2014.

Drobyshev, V. N.: Glacial catastrophe of 20 September 2002 in North Osetia, Russian Jo. Earth Sci, ES4004, https://doi.org/doi:10.2205/2006ES000207, 2006.

Dunse, T., Schellenberger, T., Hagen, J. O., Kääb, A., Schuler, T. V., and Reijmer, C. H.: Glacier-surge mechanisms promoted by a hydro-thermodynamic feedback to summer melt, Cryosphere, 9, 197-215, https://doi.org/10.5194/tc-9-197-2015, 2015.

Dussaillant, I., Berthier, E., Brun, F., Masiokas, M., Hugonnet, R., Favier, V., Rabatel, A., Pitte, P., and Ruiz, L.: Two decades of glacier mass loss along the Andes, Nat Geosci, 12, 803-+, https://doi.org/10.1038/s41561-019-0432-5, 2019.

Evans, S. G., Bishop, N. F., Smoll, L. F., Murillo, P. V., Delaney, K. B., and Oliver-Smith, A.: A re-examination of the mechanism and human impact of catastrophic mass flows originating on Nevado Huascaran, Cordillera Blanca, Peru in 1962 and 1970, Eng Geol, 108, 96-118, https://doi.org/10.1016/j.enggeo.2009.06.020, 2009a.

Evans, S. G., Tutubalina, O. V., Drobyshev, V. N., Chernomorets, S. S., McDougall, S., Petrakov, D. A., and Hungr, O.: Catastrophic detachment and high-velocity long-runout flow of Kolka Glacier, Caucasus Mountains, Russia in 2002, Geomorphology, 105, 314-321, https://doi.org/10.1016/j.geomorph.2008.10.008, 2009b.

Evans, S. G., and Delaney, K. B.: Catastrophic mass flows in the mountain glacial environment, in: Snow and Ice-related Hazards, Risks, and Disasters, edited by: Haeberli, W., and Whitemann, C., Hazards and Disasaters Series, Elsevier, Amsterdam, 563-606, 2015, https://doi.org/10.1016/B978-0-12-394849-6.00016-0.

Faillettaz, J., Sornette, D., and Funk, M.: Numerical modeling of a gravity-driven instability of a cold hanging glacier: reanalysis of the 1895 break-off of Altelsgletscher, Switzerland, J Glaciol, 57, 817-831, 2011.

Faillettaz, J., Funk, M., and Vincent, C.: Avalanching glacier instabilities: Review on processes and early warning perspectives, Rev. Geophys., 53, 203-224, https://doi.org/10.1002/2014rg000466, 2015.

Falaschi, D., Bolch, T., Lenzano, M. G., Tadono, T., Lo Vecchio, A., and Lenzano, L.: New evidence of glacier surges in the Central Andes of Argentina and Chile, Prog Phys Geog, 42, 792-825, https://doi.org/10.1177/0309133318803014, 2018a.

Falaschi, D., Lenzano, M. G., Tadono, T., Vich, A., and Lenzano, L.: Balance de masa geodésico 2000-2011 de los glaciares de la cuenca del río Atuel, Andes Centrales de Mendoza, Geoacta, 42, 7-22, 2018b.

Falaschi, D., Kääb, A., Paul, F., Tadono, T., Rivera, J. A., and Lenzano, L. E.: Brief communication: Collapse of 4 Mm(3) of ice from a cirque glacier in the Central Andes of Argentina, Cryosphere, 13, 997-1004, https://doi.org/10.5194/tc-13-997-2019, 2019.

Fischer, L., Huggel, C., Kääb, A., and Haeberli, W.: Slope failures and erosion rates on a glacierized high-mountain face under climatic changes, Earth Surf. Proc. Land., 38, 836-846, https://doi.org/10.1002/Esp.3355, 2013.

Flowers, G. E., Jarosch, A. H., Belliveau, P. T. A. P., and Fuhrman, L. A.: Short-term velocity variations and sliding sensitivity of a slowly surging glacier, Ann Glaciol, 57, 71-83, https://doi.org/10.1017/aog.2016.7, 2016.

Fowler, A. C., Murray, T., and Ng, F. S. L.: Thermally controlled glacier surging, J Glaciol, 47, 527-538, https://doi.org/Doi 10.3189/172756501781831792, 2001.

https://doi.org/10.5194/tc-2020-243
Preprint. Discussion started: 22 October 2020

1022 Frappe, T. P., and Clarke, G. K. C.: Slow surge of Trapridge Glacier, Yukon territory, Canada, J Geophys Res-Earth, 112, Artn F03s32, https://doi.org/10.1029/2006jf000607, 2007.

1024 Gardelle, J., Berthier, E., Arnaud, Y., and Kääb, A.: Region-wide glacier mass balances over the Pamir-Karakoram-Himalaya during 1999-2011, Cryosphere, 7, 1263-1286, 2013.

1026 Gilbert, A., Leinss, S., Kargel, J., Kääb, A., Gascoin, S., Leonard, G., Berthier, E., Karki, A., and Yao, T. D.: Mechanisms leading to the 2016 giant twin glacier collapses, Aru Range, Tibet, Cryosphere, 12, 2883-2900, 1028 https://doi.org/10.5194/tc-12-2883-2018, 2018.

Gruber, F. E., and Mergili, M.: Regional-scale analysis of high-mountain multi-hazard and risk indicators in the Pamir 1030 (Tajikistan) with GRASS GIS, Nat Hazard Earth Sys, 13, 2779-2796, https://doi.org/10.5194/nhess-13-2779-2013, 2013.

1032 Haeberli, W., Kääb, A., Paul, F., Chiarle, M., Mortara, G., Mazza, A., and Richardson, S.: A surge-type movement at Ghiacciaio del Belvedere and a developing slope instability in the east face of Monte Rosa, Macugnaga, Italian Alps, 1034 56, 104-111, 2002.

Haeberli, W., Huggel, C., Kaab, A., Zgraggen-Oswald, S., Polkvoj, A., Galushkin, I., Zotikov, I., and Osokin, N.: The 1036 Kolka-Karmadon rock/ice slide of 20 September 2002: an extraordinary event of historical dimensions in North Ossetia, Russian Caucasus, J Glaciol, 50, 533-546, https://doi.org/Doi 10.3189/172756504781829710, 2004.

1038 Harrison, W. D., and Post, A. S.: How much do we really know about glacier surging?, Ann Glaciol, 36, 1-6, https://doi.org/Doi 10.3189/172756403781816185, 2003.

1040 Harrison, W. D., Osipova, G. B., Nosenko, G. A., Espizua, L., Kääb, A., Fischer, L., Huggel, C., Craw Burns, P. A., Truffer, M., and Lai, A. W.: Glacier Surges, in: Snow and Ice-related Hazards, Risks, and Disasters, edited by: Haeberli, W., 1042 and Whitemann, C., Elsevier, Amsterdam, 437-485, 2015.

Hauser, A.: Rock avalanche and resulting debris flow in Estero Parraguirre and Río Colorado, Región Metropolitana, Chile, 1044 in: Catastrophic Landslides: Effects, Occurrence, and Mechanisms, edited by: Evans, S. G., and DeGraff, J. V., Geological Society of America Reviews in Engineering Geology 15, Boulder, CO, 135-148, 2002.

1046 Herreid, S., and Truffer, M.: Automated detection of unstable glacier flow and a spectrum of speedup behavior in the Alaska Range, J Geophys Res-Earth, 121, 64-81, https://doi.org/10.1002/2015jf003502, 2016.

1048 Heybrock, W. Earthquakes as a Cause of Glacier Avalanches in the Caucasus. Geographical Review 25. (3): 423–429, https://doi.org/10.2307/209310, 1935.

1050 Hock, R., Rasul, G., Adler, C., Cáceres, B., Gruber, S., Hirabayashi, Y., Jackson, M., Kääb, A., Kang, S., Kutuzov, S., Milner, A., Molau, U., Morin, S., Orlove, B., and Steltzer, H.: High Mountain Areas, in: IPCC Special Report on the 1052 Ocean and Cryosphere in a Changing Climate (SROCC), edited by: Pörtner, H.-O., Roberts, D. C., Masson-Delmotte, V., Zhai, P., Tignor, M., Poloczanska, E., Mintenbeck, E., Alegría, A., Nicolai, M., Okem, A., Petzold, J., Rama, B., 1054 and Weyer, N. M., IPCC, Geneva, 2019.

Hoinkes, H.: Die Ausbrüche (surges) des Kolka-Gletschers in Nord-Ossetien, Zentraler Kaukasus, Z. Gletscherkd. Glazial-1056 geol., 253-270, 1972.

Hu, K. H., Zhang, X. P., You, Y., Hu, X. D., Liu, W. M., and Li, Y.: Landslides and dammed lakes triggered by the 2017 1058 Ms6.9 Milin earthquake in the Tsangpo gorge, Landslides, 16, 993-1001, https://doi.org/10.1007/s10346-019-01168-w, 2019.

1060 Huggel, C., Zgraggen-Oswald, S., Haeberli, W., Kääb, A., Polkvoj, A., Galushkin, I., and Evans, S. G.: The 2002 rock/ice avalanche at Kolka/Karmadon, Russian Caucasus: assessment of extraordinary avalanche formation and mobility, and 1062 application of QuickBird satellite imagery, Nat. Hazard. Earth Sys., 5, 173-187, https://doi.org/10.5194/nhess-5-173-2005, 2005.

1064 Huggel, C., Caplan-Auerbach, J., Waythomas, C. F., and Wessels, R. L.: Monitoring and modeling ice-rock avalanches from ice-capped volcanoes: A case study of frequent large avalanches on Iliamna Volcano, Alaska, J Volcanol Geoth Res, 1066 168, 114-136, https://doi.org/10.1016/j.jvolgeores.2007.08.009, 2007.

https://doi.org/10.5194/tc-2020-243
Preprint. Discussion started: 22 October 2020

Huggel, C.: Recent extreme slope failures in glacial environments: effects of thermal perturbation, Quaternary Sci Rev, 28, 1119-1130, https://doi.org/10.1016/j.quascirev.2008.06.007, 2009.

Iribarren Anacona, P., Mackintosh, A., and Norton, K. P.: Hazardous processes and events from glacier and permafrost areas: lessons from the Chilean and Argentinean Andes, Earth Surf Proc Land, 40, 2-21, https://doi.org/10.1002/esp.3524, 2015.

Jacquemart, M., and Loso, M.: Catastrophic glacier collapse and debris flow at Flat Creek, Wrangell-St. Elias National Park and Preserve. Alaska Park Science 18(1): 16-25., 18, 16-25, 2019.

Jacquemart, M., Loso, M., Leopold, M., Welty, E., Berthier, E., Hansen, J. S. S., Sykes, J., and Tiampo, K.: What drives large-scale glacier detachments? Insights from Flat Creek glacier, St. Elias Mountains, Alaska, Geol, https://doi.org/10.1130/g47211.1, 2020.

Jiskoot, H.: Glacier surging, in: Encyclopedia of Snow, Ice and Glaciers, edited by: Singh, V. P., and Haritashya, U. K., Springer, 415-428, 2011.

Kamb, B.: Glacier surge mechanism based on linked cavity configuration of the basal water conduit system, J Geophys Res-Solid, 92, 9083-9100, https://doi.org/Doi 10.1029/Jb092ib09p09083, 1987.

Khatisyan, G. S. The Kazbek glaciers in the period from 1862 to 1887. Izvestiya Imperatorskago Russkago Geograficheskago Obschestva 24(5): 326-347 (in Russian), 1889.

Kochtitzky, W., Jiskoot, H., Copland, L., Enderlin, E., Mcnabb, R., Kreutz, K., and Main, B.: Terminus advance, kinematics and mass redistribution during eight surges of Donjek Glacier, St. Elias Range, Canada, 1935 to 2016, J Glaciol, 65, 565-579, https://doi.org/10.1017/jog.2019.34, 2019.

Kotlyakov, V. M., Rototaeva, O. V., and Nosenko, G. A.: The September 2002 Kolka glacier catastrophe in North Ossetia, Russian Federation. Evidence and analysis, Mt Res Dev, 24, 78-83, 2004.

Kotlyakov, V. M., Osipova, G. B., and Tsvetkov, D. G.: Monitoring surging glaciers of the Pamirs, central Asia, from space, 48, 125-134, https://doi.org/10.3189/172756408784700608, 2008.

Kotlyakov, V. M., Osipova, G. B., and Tsvetkov, D. G.: Investigations of the fluctuations of surge-type glaciers in the Pamir based on observations from space, in: Glaciers of Asia, U.S. Geological Survey Professional Paper 1386, edited by: Williams, R. S. J., and Ferrigno, J. G., USGS, 77-93, 2010a.

Kotlyakov, V. M., Rototaeva, O. V., and Nosenko, G. A.: Fluctuations of Glaciers of the Central Caucasus and Gora El'brus, with a Section on the Glaciological Disaster in North Osetiya, in: Glaciers of Asia, U.S. Geological Survey Professional Paper 1386, edited by: Williams, R. S. J., and Ferrigno, J. G., USGS, 59-76, 2010b.

Kutuzov, S., Lavrentiev, I., Smimov, A., Nosenko, G., and Petrakov, D.: Volume Changes of Elbrus Glaciers From 1997 to 2017, Front Earth Sc-Switz, 7, https://doi.org/UNSP 153, 10.3389/feart.2019.00153, 2019.

Kääb, A., Huggel, C., Barbero, S., Chiarle, M., Cordola, M., Epifani, F., Haeberli, W., Mortara, G., Semino, P., Tamburini, A., and Viazzo, G.: Glacier hazards at Belvedere Glacier and the Monte Rosa east face, Italian Alps: processes and mitigation, Interpraevent, 2004, 67-78,

Kääb, A., Treichler, D., Nuth, C., and Berthier, E.: Brief Communication: Contending estimates of 2003–2008 glacier mass balance over the Pamir–Karakoram–Himalaya, Cryosphere, 9, 557-564, https://doi.org/10.5194/tc-9-557-2015, 2015.

Kääb, A., Leinss, S., Gilbert, A., Buhler, Y., Gascoin, S., Evans, S. G., Bartelt, P., Berthier, E., Brun, F., Chao, W. A., Farinotti, D., Gimbert, F., Guo, W. Q., Huggel, C., Kargel, J. S., Leonard, G. J., Tian, L. D., Treichler, D., and Yao, T. D.: Massive collapse of two glaciers in western Tibet in 2016 after surge-like instability, Nat Geosci, 11, 114-120, https://doi.org/10.1038/s41561-017-0039-7, 2018.

Kääb, A.: Collapsing Glaciers, Geophysical Research Abstracts, European Geosciences Union General Assembly 2019, Vol. 21, 8799, 2019.

Larsen, C. F., Burgess, E., Arendt, A. A., O'Neel, S., Johnson, A. J., and Kienholz, C.: Surface melt dominates Alaska glacier mass balance, Geophys Res Lett, 42, 5902-5908, https://doi.org/10.1002/2015gl064349, 2015.

https://doi.org/10.5194/tc-2020-243
Preprint. Discussion started: 22 October 2020

Leinss, S., Willimann, C., and Hajnsek, I.: Glacier Detachment Hazard Analysis in the West Kunlun Shan Mountains, Int Geosci Remote Se, 4565-4568, 2019.

Leinss, S., Bernardini, E., Jacquemart, M., and Dokukin, M.: Glacier detachments and rock-ice avalanches in the Petra Pervogo range, Tajikistan (1973–2019), Nat. Hazards Earth Syst. Sci. Discuss., https://doi.org/10.5194/nhess-2020-285, in review, 2020.

Liu, C. Z., Lu, J. T., Tong, L. Q., Chen, H. Q., Liu, Q. Q., Xiao, R. H., and Tu, J. N.: Research on glacial/rock fall-landslide-debris flows in Sedongpu basin along Yarlung Zangbo River in Tibet, Geol. China, 46, 219-234, 2019.

Lv, M. Y., Guo, H. D., Lu, X. C., Liu, G., Yan, S. Y., Ruan, Z. X., Ding, Y. X., and Quincey, D. J.: Characterizing the behaviour of surge-and non-surge-type glaciers in the Kingata Mountains, eastern Pamir, from 1999 to 2016, Cryosphere, 13, 219-236, https://doi.org/10.5194/tc-13-219-2019, 2019.

Marangunic, C.: Informe sobre deslizamientos de glaciares en el Estero del Aparejo, Valle del Río Maipo, Área Metropolitana, Oficina Nacional de Emergencias, Santiago, Chile, 8p, 1980.

Masiokas, M. H., Christie, D. A., Le Quesne, C., Pitte, P., Ruiz, L., Villalba, R., Luckman, B. H., Berthier, E., Nussbaumer, S. U., Gonzalez-Reyes, A., McPhee, J., and Barcaza, G.: Reconstructing the annual mass balance of the Echaurren Norte glacier (Central Andes, 33.5 degrees S) using local and regional hydroclimatic data, Cryosphere, 10, 927-940, https://doi.org/10.5194/tc-10-927-2016, 2016.

McClung, D. M.: Superelevation of flowing avalanches around curved channel bends, J Geophys Res-Sol Ea, 106, 16489-16498, https://doi.org/Doi 10.1029/2001jb000266, 2001.

Mergili, M., Kopf, C., Mullebner, B., and Schneider, J. F.: Changes of the Cryosphere and Related Geohazards in the High-Mountain Areas of Tajikistan and Austria: A Comparison, Geogr Ann A, 94A, 79-96, https://doi.org/10.1111/j.1468-0459.2011.00450.x, 2012.

Moore, P. L.: Deformation of debris-ice mixtures, Rev Geophys, 52, 435-467, https://doi.org/10.1002/2014rg000453, 2014.

Murray, T., Strozzi, T., Luckman, A., Jiskoot, H., and Christakos, P.: Is there a single surge mechanism? Contrasts in dynamics between glacier surges in Svalbard and other regions, 108, 2237, https://doi.org/10.1029/2002JB001906, 2003.

Obu, J., Westermann, S., Bartsch, A., Berdnikov, N., Christiansen, H. H., Dashtseren, A., Delaloye, R., Elberling, B., Etzelmuller, B., Kholodov, A., Khomutov, A., Kaab, A., Leibman, M. O., Lewkowicz, A. G., Panda, S. K., Romanovsky, V., Way, R. G., Westergaard-Nielsen, A., Wu, T. H., Yamkhin, J., and Zou, D. F.: Northern Hemisphere permafrost map based on TTOP modelling for 2000-2016 at 1 km(2) scale, Earth-Sci Rev, 193, 299-316, https://doi.org/10.1016/j.earscirev.2019.04.023, 2019.

Paul, F.: Repeat Glacier Collapses and Surges in the Amney Machen Mountain Range, Tibet, Possibly Triggered by a Developing Rock-Slope Instability, Remote Sens-Basel, 11, https://doi.org/ARTN 708, 10.3390/rs11060708, 2019.

Pavez, C., Tapia, F., Comte, D., Gutierrez, F., Lira, E., Charrier, R., and Benavente, O.: Characterization of the hydrothermal system of the Tinguiririca Volcanic Complex, Central Chile, using structural geology and passive seismic tomography, J Volcanol Geoth Res, 310, 107-117, https://doi.org/10.1016/j.jvolgeores.2015.11.018, 2016.

Petrakov, D. A., Chernomorets, S. S., Evans, S. G., and Tutubalina, O. V.: Catastrophic glacial multi-phase mass movements: a special type of glacial hazard, 14, 211-218, 2008.

Petrakov, D. A., Aristov, K. A., A.A., A., Boyko, E. S., Drobyshev, V. N., Kovalenko, N. V., Tutubalina, O. V., and Chernomorets, S. S.: Rapid regeneration of the Kolka Glacier (Caucasus) after the 2002 glacial disaster Earths's Cryosphere (Kriosfera Zemli), 22, 51–62, https://doi.org/DOI: 10.21782/EC2541-9994-2018-1(51-62) 2018.

Post, A.: Effects on Glaciers, in: The great Alaska earthquake of 1964. Part A: hydrology, National Academy of Sciences, Washington DC, 266-308, 1968.

Quincey, D. J., Glasser, N. F., Cook, S. J., and Luckman, A.: Heterogeneity in Karakoram glacier surges, J Geophys Res-Earth, 120, 1288-1300, https://doi.org/10.1002/2015jf003515, 2015.

Reineggs, J. Allgemeine historisch- topographische Beschreibung des Kaukasus. - Gotha; St. Petersburg, Bd. 1, 296 S., http://elib.shpl.ru/ru/nodes/24706-bd-1-1796, 1796.

https://doi.org/10.5194/tc-2020-243
Preprint. Discussion started: 22 October 2020

Rototayev, K. P., Khodakov, V. G., and Krenke, A. N.: Study of the Surging Kolka Glacier, Nauka, Moscow, 168 pp. (in Russian), 1983.

Schneider, D., Huggel, C., Haeberli, W., and Kaitna, R.: Unraveling driving factors for large rock-ice avalanche mobility, Earth Surf. Proc. Land., 36, 1948-1966, https://doi.org/10.1002/esp.2218, 2011.

Sevestre, H., and Benn, D. I.: Climatic and geometric controls on the global distribution of surge-type glaciers: Implications for a unifying model of surging, J. Glaciol., 61, 646-662, https://doi.org/10.3189/2015JoG14J136, 2015.

Sevestre, H., Benn, D. I., Hulton, N. R. J., and Baelum, K.: Thermal structure of Svalbard glaciers and implications for thermal switch models of glacier surging, J Geophys Res-Earth, 120, 2220-2236, https://doi.org/10.1002/2015jf003517, 2015.

Shean, D. E., Bhushan, S., Montesano, P., Rounce, D. R., Arendt, A., and Osmanoglu, B.: A Systematic, Regional Assessment of High Mountain Asia Glacier Mass Balance, Front Earth Sc-Switz, 7, https://doi.org/ARTN 363, 10.3389/feart.2019.00363, 2020.

Sheridan, M. F., Stinton, A. J., Patra, A., Pitman, E. B., Bauer, A., and Nichita, C. C.: Evaluating Titan2D mass-flow model using the 1963 Little Tahoma Peak avalanches, Mount Rainier, Washington, J Volcanol Geoth Res, 139, 89-102, https://doi.org/10.1016/j.jvolgeores.2004.06.011, 2005.

Shugar, D. H., Rabus, B. T., Clague, J. J., and Capps, D. M.: The response of Black Rapids Glacier, Alaska, to the Denali earthquake rock avalanches, J Geophys Res-Earth, 117, https://doi.org/Artn F01006, 10.1029/2011jf002011, 2012.

Statkowski, B. I. Origin of repeating Kazbek blockage and measures for its prevention. Tiflis (in Russian), 1877.

Statkowski, B. Problèmes de la Climatologie du Caucase. Paris, Gauthier-Villars, Imprimeur-Librarie. Successeur de Mallet-Bachelier. 279 p. https://gallica.bnf.fr/ark:/12148/bpt6k9643218p.texteImage , 1879.

Stebnitsky, I. I. On the distribution of glaciers in the Caucasus. – Izvestiya Kavkazskogo otdela Imperatorskago Russkago Geograficheskago Obschestva, V(1): 1-21 (in Russian), 1877.

Strom, A., and Abdrakhmatov, K.: Rockslides and Rock Avalanches of Central Asia: Distribution, Morphology, and Internal Structure, Elsevier, Amsterdam, 2018.

Tavasiev, R. A., and Galushkin, I. V. Rock-ice collapse of Kazbek Mountain dated May 17, 2014. Vestnik Vladikavkaz Scientific Center, 14(2): 43-45, 2014.

Thogersen, K., Gilbert, A., Schuler, T. V., and Malthe-Sorenssen, A.: Rate-and-state friction explains glacier surge propagation, Nat Commun, 10, https://doi.org/ARTN 2823, 10.1038/s41467-019-10506-4, 2019.

Tian, L. D., Yao, T. D., Gao, Y., Thompson, L., Mosley-Thompson, E., Muhammad, S., Zong, J. B., Wang, C., Jin, S. Q., and Li, Z. G.: Two glaciers collapse in western Tibet, J Glaciol, 63, 194-197, https://doi.org/10.1017/jog.2016.122, 2017.

Tielidze, L. G., Kumladze, R. M., Wheate, R. D., and Gamkrelidze, M. The Devdoraki Glacier Catastrophes, Georgian Caucasus. Hungarian Geographical Bulletin, 68(1), 21-35, https://doi.org/10.15201/hungeobull.68.1.2, 2019.

Toney et al., 2020. Reconstructing the dynamics of the highly-similar May 2016 and June 2019 Iliamna Volcano, Alaska ice–rock avalanches from seismoacoustic data. https://doi.org/10.5194/esurf-2020-47

Tong, L. Q., Tu, J. N., Pei, L. X., Guo, Z. C., Zheng, X. W., Fan, J. H., Zhong, X., Liu, C. L., Wang, S. S., He, P., and Chen, H.: Preliminary discussion of the frequent debris flow events in Sedongpu Basin at Gyala Peri peak, Yarlung Zangbo River, J. Eng.Geol., 26, 1552-1561, https://doi.org/10.13544/j.cnki.jeg.2018-401, 2018.

Treichler, D., Kääb, A., Salzmann, N., and Xu, C. Y.: Recent glacier and lake changes in High Mountain Asia and their relation to precipitation changes, Cryosphere, 13, 2977-3005, https://doi.org/10.5194/tc-13-2977-2019, 2019.

Truffer, M., Harrison, W. D., and Echelmeyer, K. A.: Glacier motion dominated by processes deep in underlying till, J Glaciol, 46, 213-221, https://doi.org/Doi 10.3189/172756500781832909, 2000.

Ugalde, F., Casassa, G., Marangunic, C., Mujica, R., and Peralta, C.: El deslizamiento catastrófico del glaciar Aparejo: 35 años después, XiV Congreso Geologico Chileno, 2015,

https://doi.org/10.5194/tc-2020-243
Preprint. Discussion started: 22 October 2020

Ugalde, F., Marangunic, C., and Casassa, G.: Ice thickness changes at Aparejo Glacier in central Chile from interferometric satellite data, 76-79, 2017.

Ugalde, F. I. P.: ESTIMACIÓN DE PELIGRO ANTE DESLIZAMIENTO DE GLACIARES EN CHILE CENTRAL: EL CASO DEL GLACIAR APAREJO, DEPARTAMENTO DE GEOLOGÍA, FACULTAD DE CIENCIAS FÍSICAS Y MATEMÁTICAS , UNIVERSIDAD DE CHILE SANTIAGO DE CHILE, 2016.

van der Woerd, J., Owen, L. A., Tapponnier, P., Xu, X. W., Kervyn, F., Finkel, R. C., and Barnard, P. L.: Giant, similar to M8 earthquake-triggered ice avalanches in the eastern Kunlun Shan, northern Tibet: Characteristics, nature and dynamics, Geol Soc Am Bull, 116, 394-406, https://doi.org/10.1130/B25317.1, 2004.

Viskovatov, A. A. About periodic Kazbek blockage. Zapiski Kavkazskago otdela Imperatorskago Russkago geograficheskago obshestva 6: 186-219. Tiflis (in Russian), 1864.

Wagner, S.: Dreidimensionale Modellierung zweier Gletscher und Deformationsanalyse von eisreichem Permafrost. Mitteilungen der Versuchsanstalt für Wasserbau, Hydrologie und Glaziologie der ETH Zürich, 146, 135pp, 1996.

Wenying, W.: Glaciers in the north-eastern part of the Ch'ing-hai–hsi-tsang (Qinghai–Xizang) Plateau (Tibet) and their variations, J Glaciol, 29, 383-391, 1983.

Zaporozhchenko, E. V., and Chernomorets, S. S. History and studies of Kazbek blockages. Vestnik Kavkazskogo gornogo obshestva 5: 33-54 https://istina.msu.ru/download/8871273/1k5k36:x_gHoGej2TQCeFRBrQCnhJLg7eU/ (in Russian), 2004.

Zemp, M., Huss, M., Thibert, E., Eckert, N., McNabb, R., Huber, J., Barandun, M., Machguth, H., Nussbaumer, S. U., Gartner-Roer, I., Thomson, L., Paul, F., Maussion, F., Kutuzov, S., and Cogley, J. G.: Global glacier mass changes and their contributions to sea-level rise from 1961 to 2016, Nature, 568, 382-+, https://doi.org/10.1038/s41586-019-1071-0, 2019.

Zhang, W. J.: Identification of Glaciers with Surge Characteristics on the Tibetan Plateau, Ann Glaciol, 16, 168-172, 1992.

Simple force balance

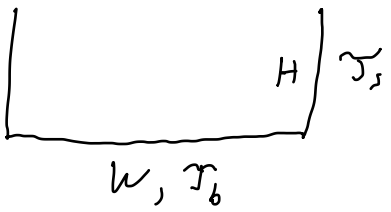

$$HW\rho g \sin\alpha = W\tau_b + 2H\tau_s$$

$$\tau_s = \frac{W}{2H}\rho g \sin\alpha - \frac{W}{2H}\tau_b$$

$\frac{W}{2H}$: half-width to depth ratio

$\sin\alpha$: slope

Maximum side stress occurs for $\tau_b = 0$

If $\tau_{s,max} \geq$ failure strength

$\Rightarrow$ detachment

otherwise: rapid flow or surge

till bed: $\tau_b = N \cdot \tan\phi$

$\tan\phi$ smaller for fine grained till

hard bed: more unlikely to achieve $N = 0$ on large spatial scale because increased bed separation would lead to more pathways for water to drain

soft bed: large scale areas of low N are easier to achieve, particularly combined with distributed water sources, such as increased geothermal heat

Influence of sudden mass addition (rock fall)

$$\Delta\tau_d = \rho_r h_r g \sin\alpha$$

$$\Delta\tau_b = \underbrace{\rho_r h_r g \cos\alpha}_{\Delta N} \cdot \tan\phi$$

$$\frac{\Delta\tau_b}{\Delta\tau_d} = \frac{\tan\alpha}{\tan\phi}$$

If $\Delta\tau_b/\Delta\tau_d < 1$ then rock fall leads to more unstable configuration

Also, over time if water pressure increases and N decreases, instability can occur